Semiannual Report for

NUMERICAL METHODS FOR ANALYZING ELECTROMAGNETIC SCATTERING

March 25, 1984 to September 24, 1984

Submitted to

Dr. Y. C. Cho

National Aeronautics and Space Administration
Lewis Research Center (MS 54-3)
Cleveland, OH 44113

Grant No. NAG-3-475

Prepared by

Professors S. W. Lee, Y. T. Lo and S. L. Chuang

Electromagnetics Laboratory
Department of Electrical and Computer Engineering
University of Illinois
Urbana, IL 61801

September 24, 1984

Semiannual Report for

NUMERICAL METHODS FOR ANALYZING ELECTROMAGNETIC SCATTERING

March 25, 1984 to September 24, 1984

Submitted to

Dr. Y. C. Cho

National Aeronautics and Space Administration
Lewis Research Center (MS 54-3)
Cleveland, OH 44113

Grant No. NAG-3-475

Prepared by

Professors S. W. Lee, Y. T. Lo and S. L. Chuang

Electromagnetics Laboratory
Department of Electrical and Computer Engineering
University of Illinois
Urbana, IL 61801

September 24, 1984

TABLE OF CONTENTS

LIST OF FIGURES

Figure Page

I. INTRODUCTION

The research grant NAG 3-475 entitled "Numerical Methods for Analyzing Electromagnetic Scattering" was awarded to the University of Illinois by NASA-Lewis Research Center on September 28, 1983. Dr. Y. C. Cho of NASA's Microwave Amplifier Section is the Technical Officer, and Mr. Boyd M. Bane is the contracting officer. The total amount of funds received by the University is

$$\$22,385 + \$52,600 = \$74,985$$

to cover the period from

September 25, 1983 to November 25, 1984 (14 months).

This report is the second semiannual report for the period March 25, 1984 to September 24, 1984.

II. TECHNICAL PERSONNEL

S. W. Lee	Professor of Electrical and Computer Engineering
Y. T. Lo	Professor of Electrical and Computer Engineering
S. L. Chuang	Assistant Professor of Electrical and Computer Engineering
C. S. Lee	Research Assistant of the Department of Electrical and Computer Engineering

III. PRESENTATION AND PUBLICATIONS

1. Professors S. W. Lee, Y. T. Lo and S. L. Chuang traveled to NASA Lewis on May 4, 1984 to present a talk entitled "Modes in Circular Guide Coated with Lossy Dielectric." Viewgraphs of the presentation are published as Electromagnetic Laboratory Report 84-1 under the same title.

2. S. L. Chuang, S. W. Lee and Y. C. Cho, "Approximate Solutions for Reflection from an Open-ended Waveguide," 1984 IEEE AP-S/URSI Symposium, Boston, MA, June 25-28, 1984.

3. C. S. Lee, S. L. Chuang and S. W. Lee, "Wave Attenuation and Mode Dispersion in a Waveguide Coated with Lossy Dielectric Material," paper presented in the Sixth Annual Workshop of the Industrial Affiliates Program on Communication, Antennas, and Propagation (CAP), Urbana-Champaign, IL, April 5-6, 1984.

4. C. S. Lee, S. W. Lee and S. L. Chuang, "Plot of modal field disribution in rectangular and circular waveguides," submitted for publication to IEEE Trans. Microwave Theory Tech.

5. C. S. Lee, S. L. Chuang, S. W. Lee, and Y. T. Lo, "Wave attenuation and mode dispersion in a waveguide coated with lossy dielectric material," Univ. of Illinois Electromagnetics Laboratory, Urbana, IL, Technical Report No. 84-13, July 1984.

IV. TECHNICAL PROGRESS

Abstract

Major items accomplished in this reporting period are:

(1) We have extended our previous approach to the high frequency case for calculating attenuation coefficients and propagation constants of a dielectric-coated circular waveguide.

(2) The magnetic-material coating has been studied. It is found that at low frequency (cylinder diameter is 2 wavelengths or less), a one-way 3 dB attenuation can be achieved within a longitudinal distance of one diameter. This is a drastic improvement over the previous "best" result

(using dielectric material), in which 17 diameters are needed for the same attenuation.

(3) We have generated a software program to plot the field patterns of the lowest 30 modes in the cylindrical waveguides.

Details are explained below.

For the first six months of this project, we studied the wave attenuation in a cylindrical waveguide coated with lossy dielectric material (Figure 1) [1]. Due to a numerical difficulty in the computer programming, the results were limited to low frequency.

In the past six-month period, we extended our scope to the high-frequency region, and we also investigated the properties of the wave attenuation in the waveguide coated with lossy magnetic material.

The method of approach is similar to that in the previous report [1] except that the functions related to Bessel functions are modified to accommodate the high-frequency problem.

In the lossy waveguide, the modes are no longer pure TE or TM. By convention, the normal modes corresponding to the TE and TM in the homogeneous waveguide are called HE and EH, respectively [2]. In this report, we will use TE and TM for the normal modes in the perfect waveguide without coating.

At high frequency, many higher-order modes are excited. Even though the field patterns of the higher-order modes are needed in many occasions in microwave research, we could not find them in the literature. Thus we spent some time to plot them. The detailed electric and magnetic field patterns are shown in Figures 2 and 3.

When the cylinder is illuminated by a plane wave nearly normal to the aperture of the cylinder, the modes with the angular index of 1 (i.e., cos ϕ

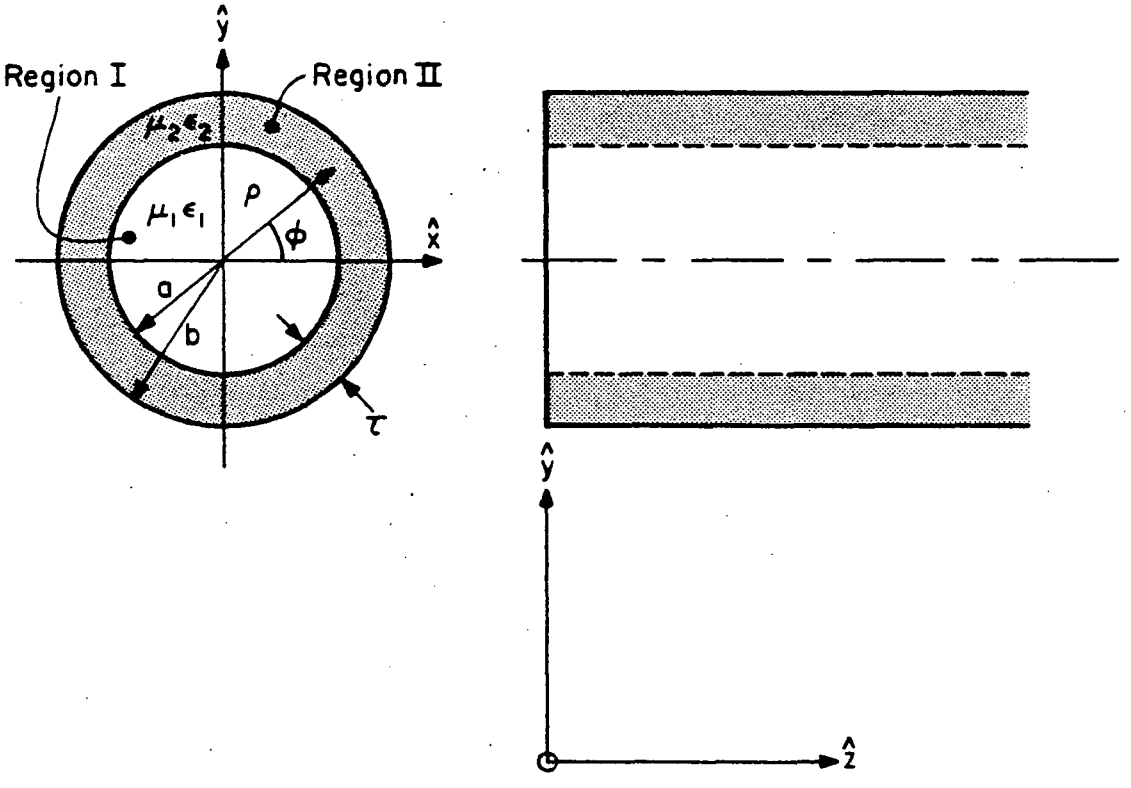

Figure 1. A cylindrical waveguide coated with a lossy material.

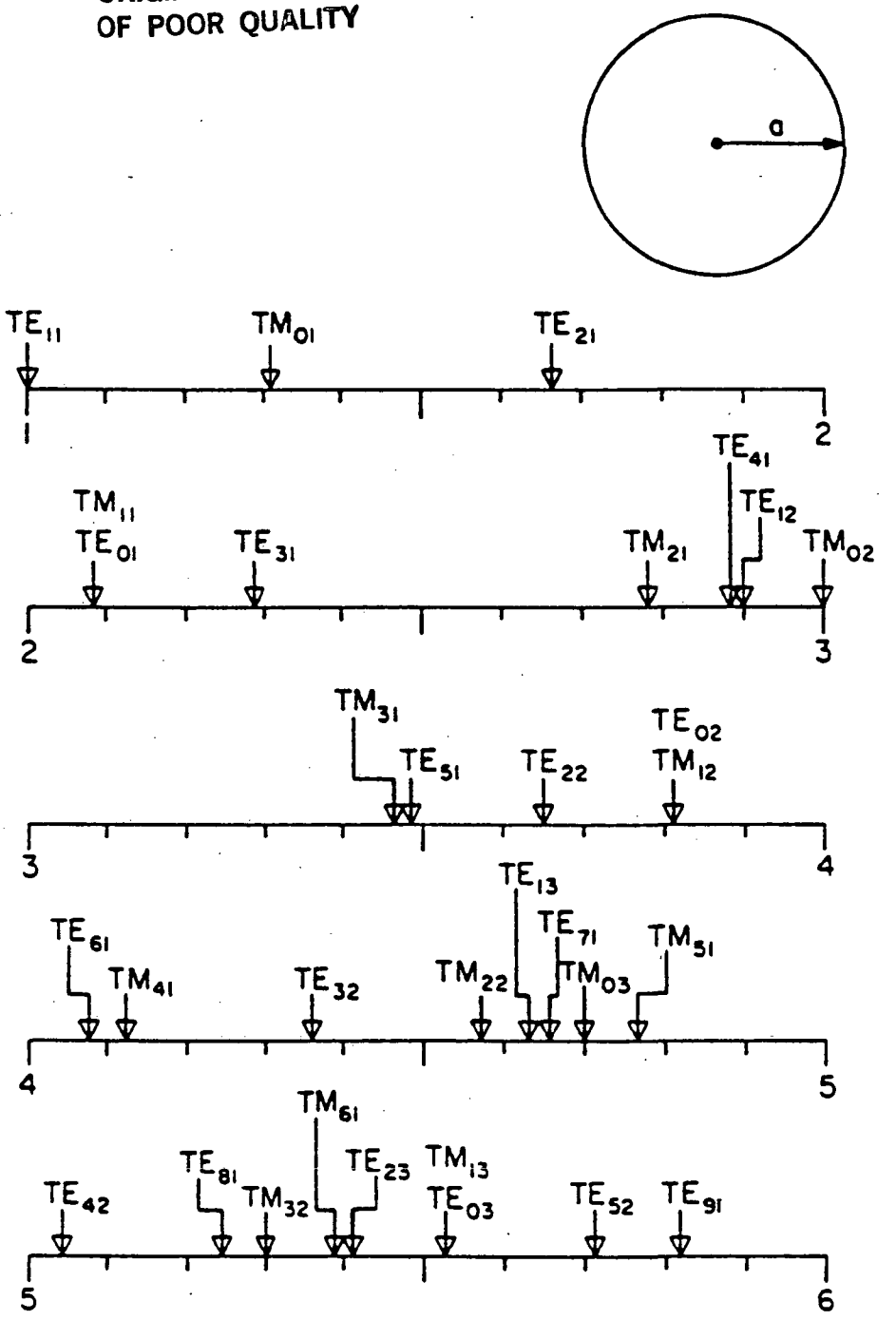

Figure 2. The ratios of cutoff frequencies of lower-order modes to the cutoff frequency of the dominant mode (TE_{11}) in a circular waveguide.

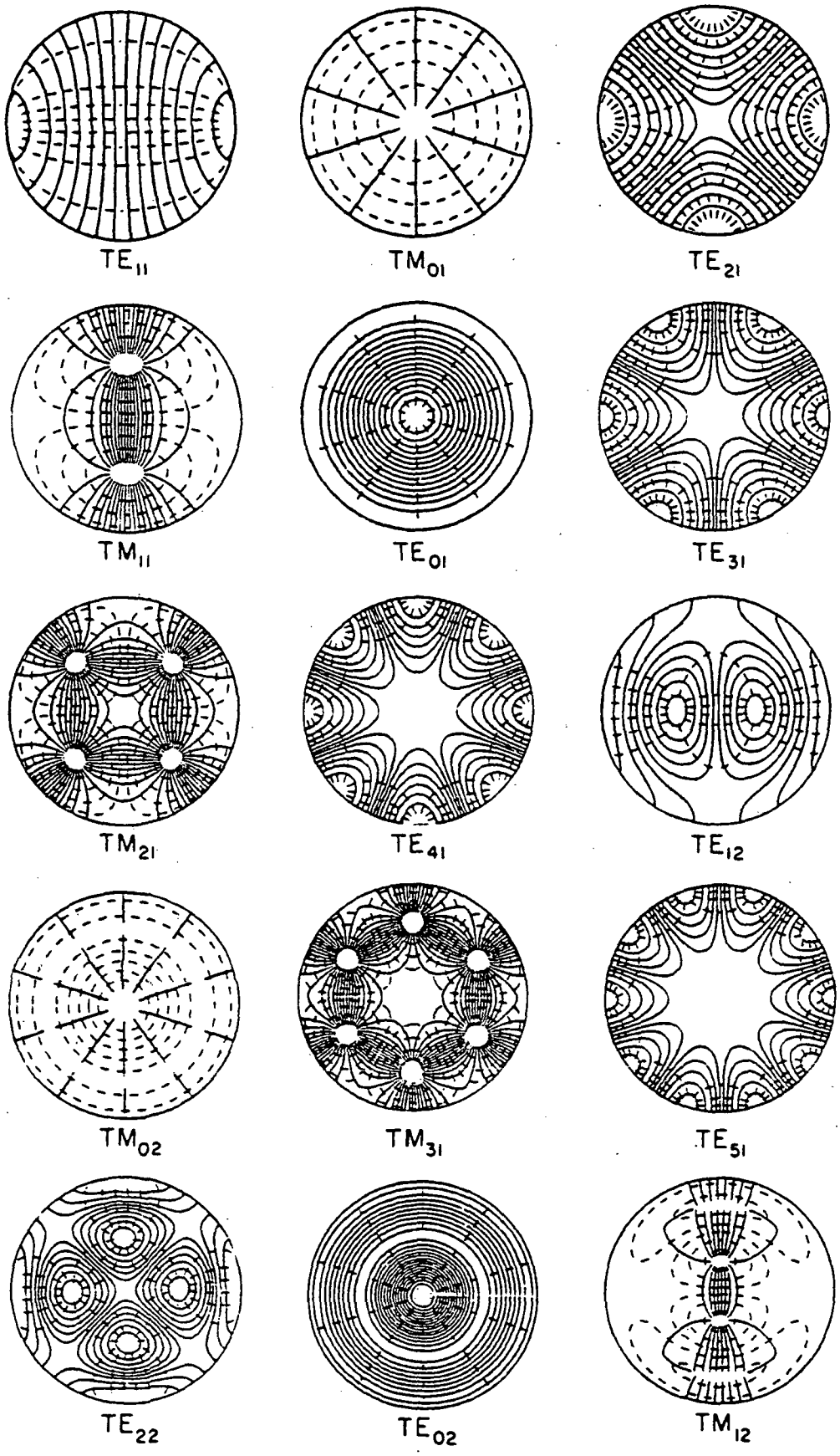

Figure 3a. Mode patterns of the first 15 lowest modes in a circular waveguide.

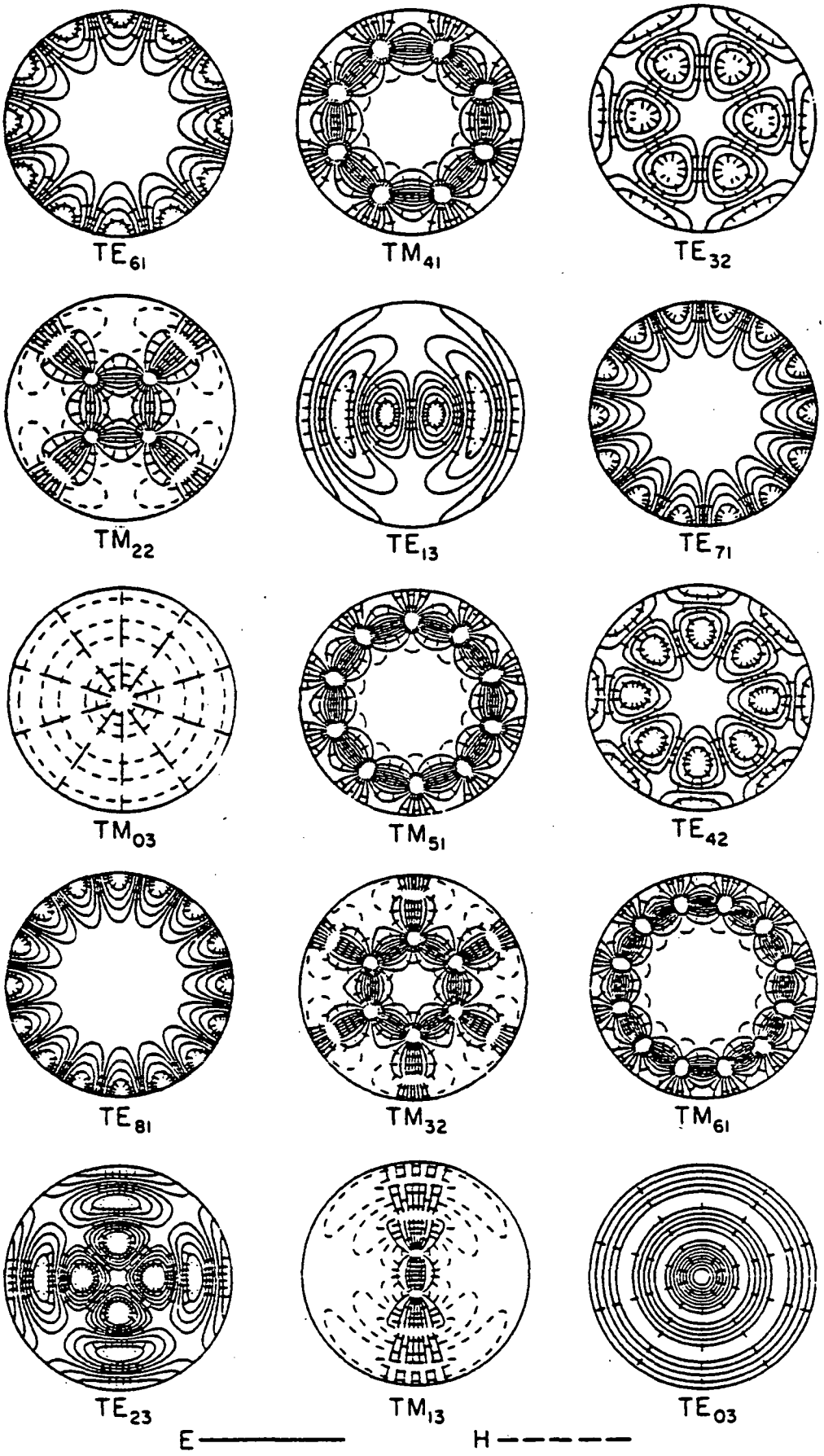

Figure 3b. Mode patterns of the second 15 lowest modes in a circular wave guide.

or sin ϕ dependence) are most strongly excited. In fact, when the perfect cylindrical waveguide is illuminated by a normally incident plane wave, only TE_{1n} modes (n = 1,2,3,...) are excited [3], [4]. When the waveguide is coated with lossy materials, the TE and TM modes are mixed to produce hybrid modes, HE and EH modes. In this case, both HE_{1n} and EH_{1n} (n = 1,2,...) are excited by the normally incident plane wave. In this report, we limit our scope to only those three lowest normal modes, namely, HE_{11}, EH_{11} and HE_{12}. We found that the properties of the normal modes with the angular indices m different from 1 are very similar to those with m = 1.

In this report, we concentrate the wave attenuation in a thinly coated waveguide. Unless specified otherwise, we assume that the outer radius b is 10 cm and the inner radius a is 9.7 cm. Thus the coating thickness is 3% of the radius.

The attenuation constants α's for those three modes (HE_{11},EH_{11} and HE_{12}) as a function of frequency are shown in Figure 4, including the high-frequency region, which was not covered in the previous report [1]. Figures 5 and 6 show the real parts, β's, of the propagation constants k_z. In these figures, the β's are normalized to the free-space wave number. Note that negative slope in these figures does not mean negative group velocity. At high frequency, the β's of the normal modes are usually very close to one another and very difficult to distinguish graphically. In this case, the normalized propagation constants illustrate the differences among those normal modes better than the unnormalized propagation constants, because we can expand the clustered region to a larger scale (Figure 6). From these figures (Figures 4, 5 and 6), we observe that the α of the HE_{11} becomes very large and the modal inversions between modes occur at the high frequency.

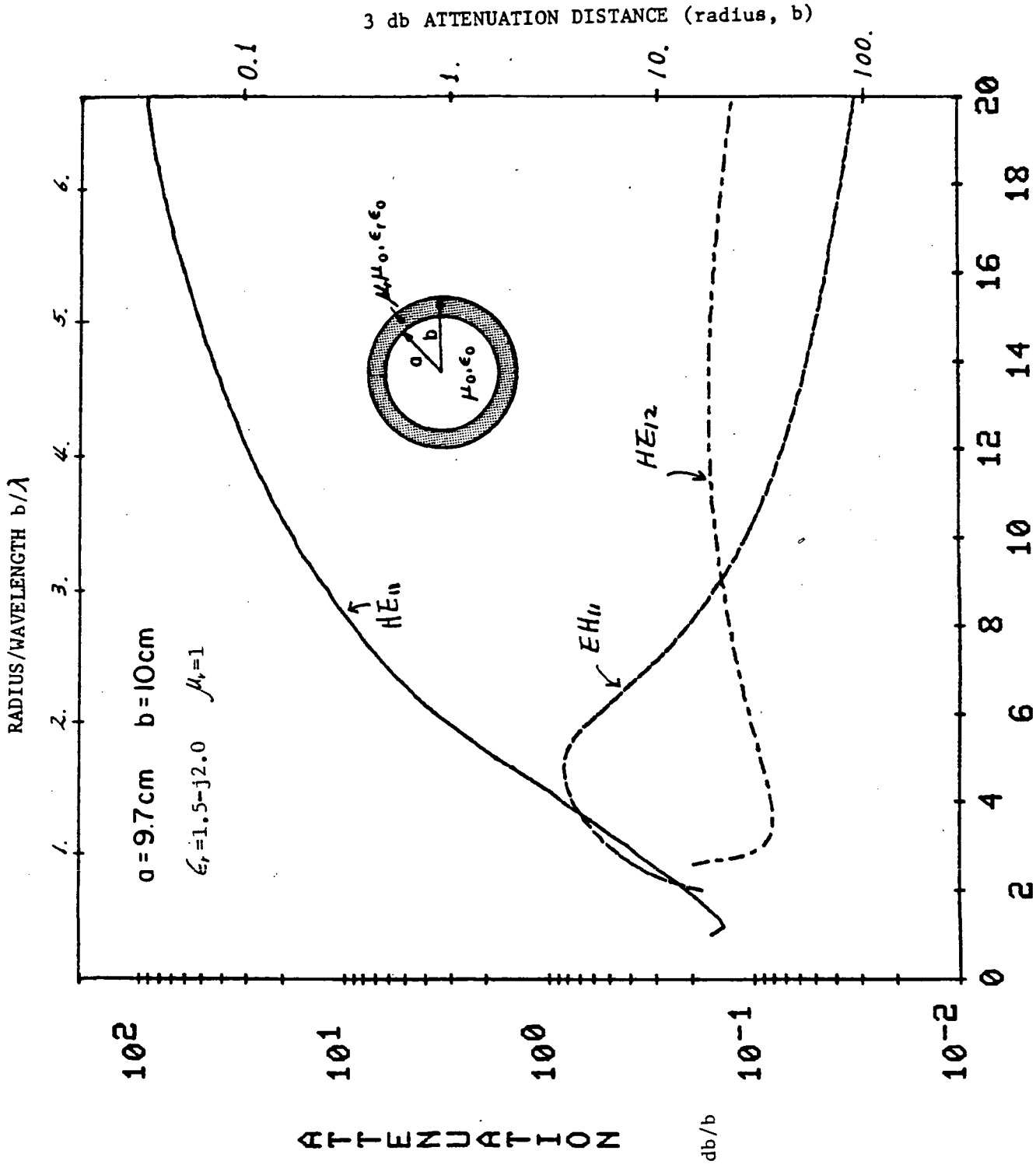

Figure 4. Attenuation constants as a function of frequency (ϵ_r = 1.5 - j2.0).

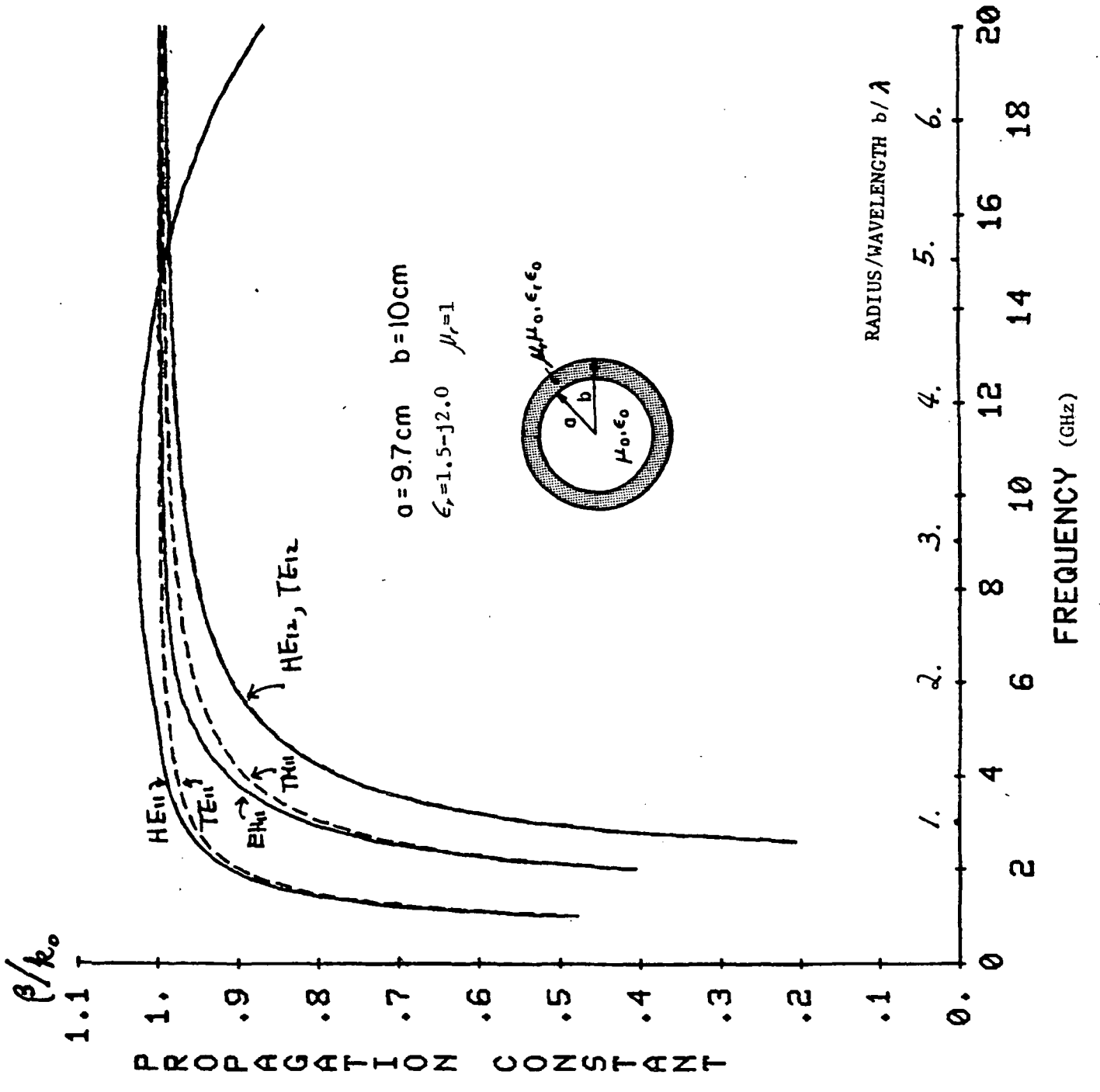

Figure 5. Normalized real parts of propagation constants as a function of frequency (ϵ_r = 1.5 - j2.0).

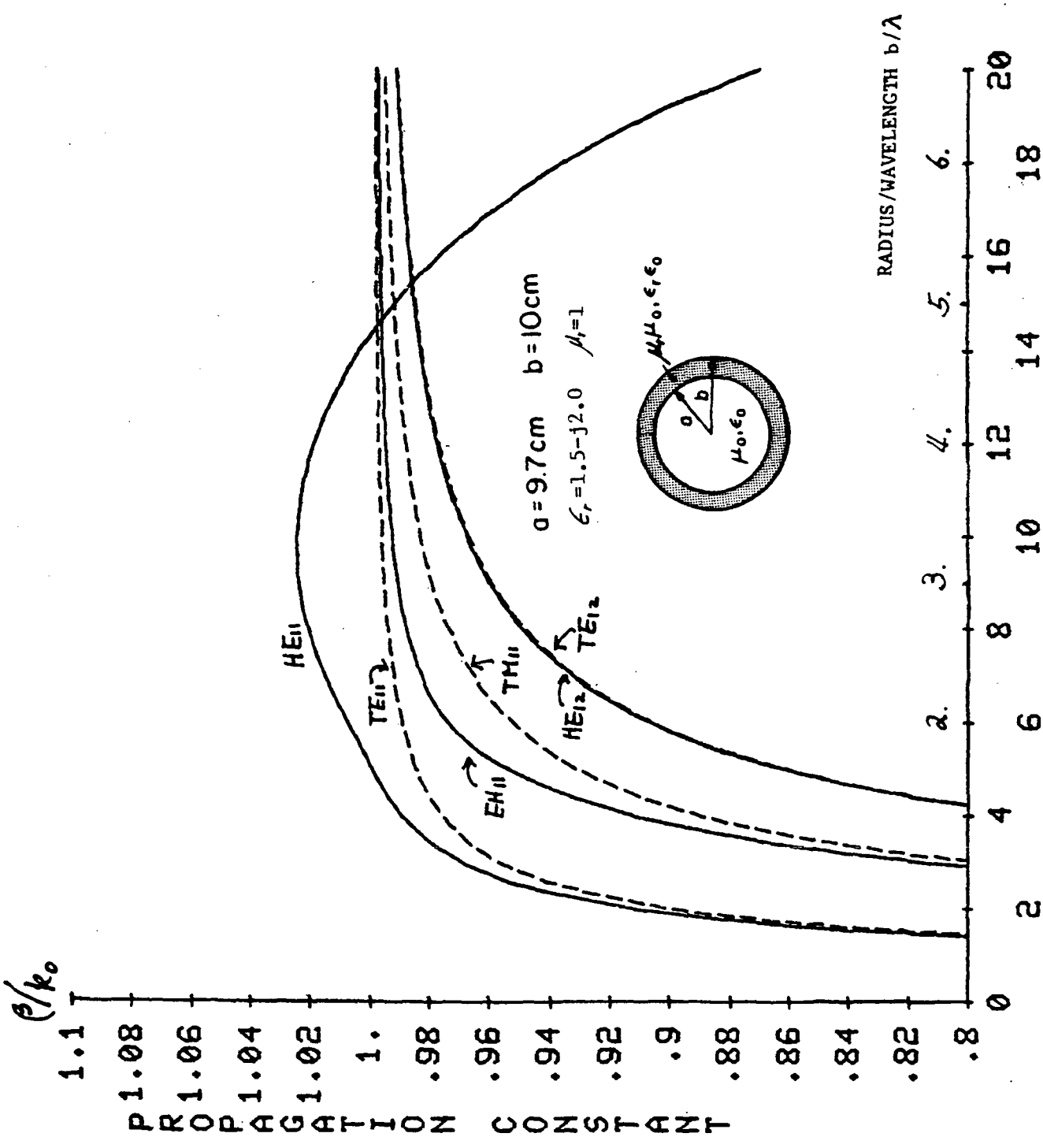

Figure 6. Normalized real parts of propagation constants as a function of frequency (detail) (ε_r = 1.5 - j2.0).

Note that at the high frequency the EH_{11} becomes the dominant mode and the influence of the HE_{11} on the overall wave attenuation decreases, because the dominant mode carries a large fraction of the transmitted power.

The modal inversions in the partially filled waveguide as frequency varies are not new. These have been reported in the literature [5], [6].

We found that the lossy dielectric with a large loss tangent is a good choice for the coating material to obtain a large wave attenuation within the waveguide [1], [4]. We have selected two promising materials for further analysis, which are polystyrene 70% and carbon 30% ($\varepsilon_r = 9.1 - j2.275$), and Catalin 700 base ($\varepsilon_r = 4.74 - j0.7252$) [7]. The α and β for polystyrene 70% and carbon 30% are shown in Figures 7, 8 and 9, and those for Catalin 700 base in Figures 10, 11 and 12. Even though two materials have quite different dielectric constants, the general patterns of the α's and β's of these two materials are very similar. Note that the HE_{11} modes become the surface modes at the high frequency. We can see this fact from the patterns of the β's (Figures 8 and 10), that is, the propagation constants are nearly equal to those of the lossy dielectric material at the high frequency. These phenomena are not present in the previous hypothetical example (Figures 5 and 6). We think this is because the magnitudes of the dielectric constants ε_r in these examples are much larger than that in the previous case ($\varepsilon_r = 1.5 - j2$, Figures 4, 5 and 6). In fact, these surface-type normal modes would not couple strongly with the incident plane wave at the aperture (as in the Kirchoff's approximation) because the fields in this case are confined to the small region of the lossy dielectric material. Thus we expect that the overall wave attenuation depends mostly on other modes, which usually have smaller attenuation constants than that of the HE_{11}.

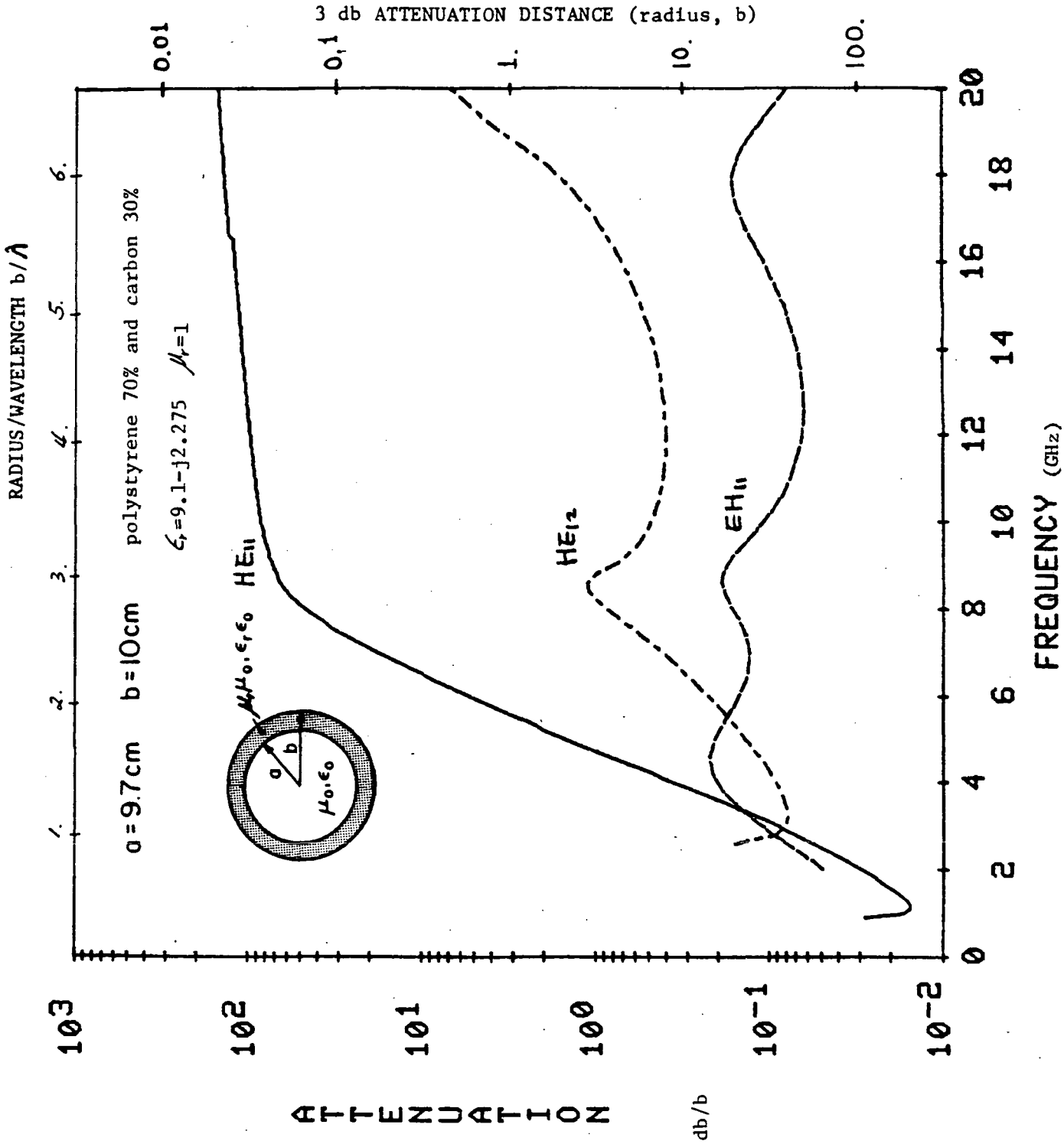

Figure 7. Attenuation constants as a function of frequency (polystyrene 70% and carbon 30%, $\varepsilon_r = 9.1 - j2.275$).

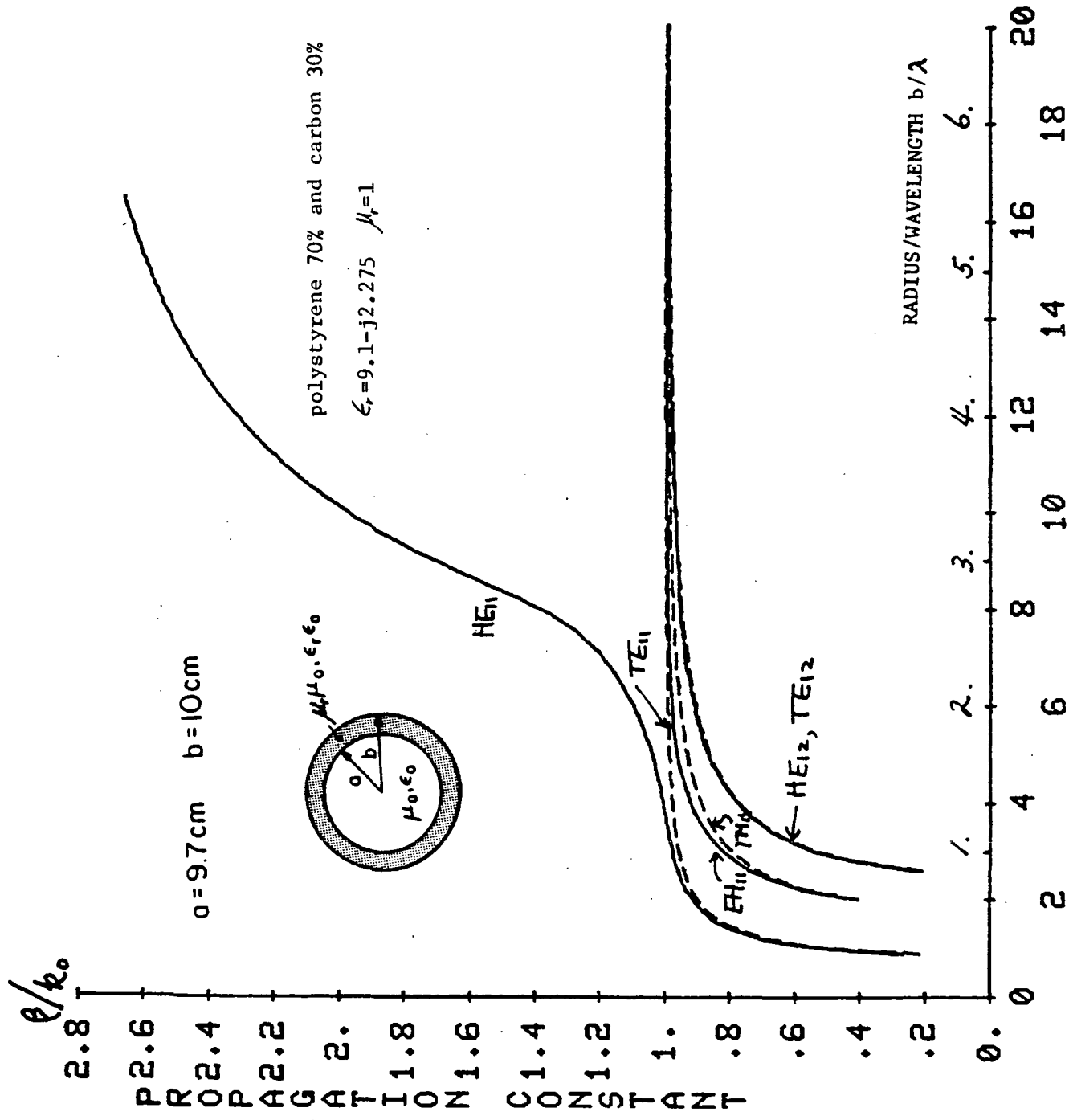

Figure 8. Normalized real parts of propagation constants as a function of frequency (polystyrene 70% and carbon 30%, $\epsilon_r = 9.1 - j2.275$)

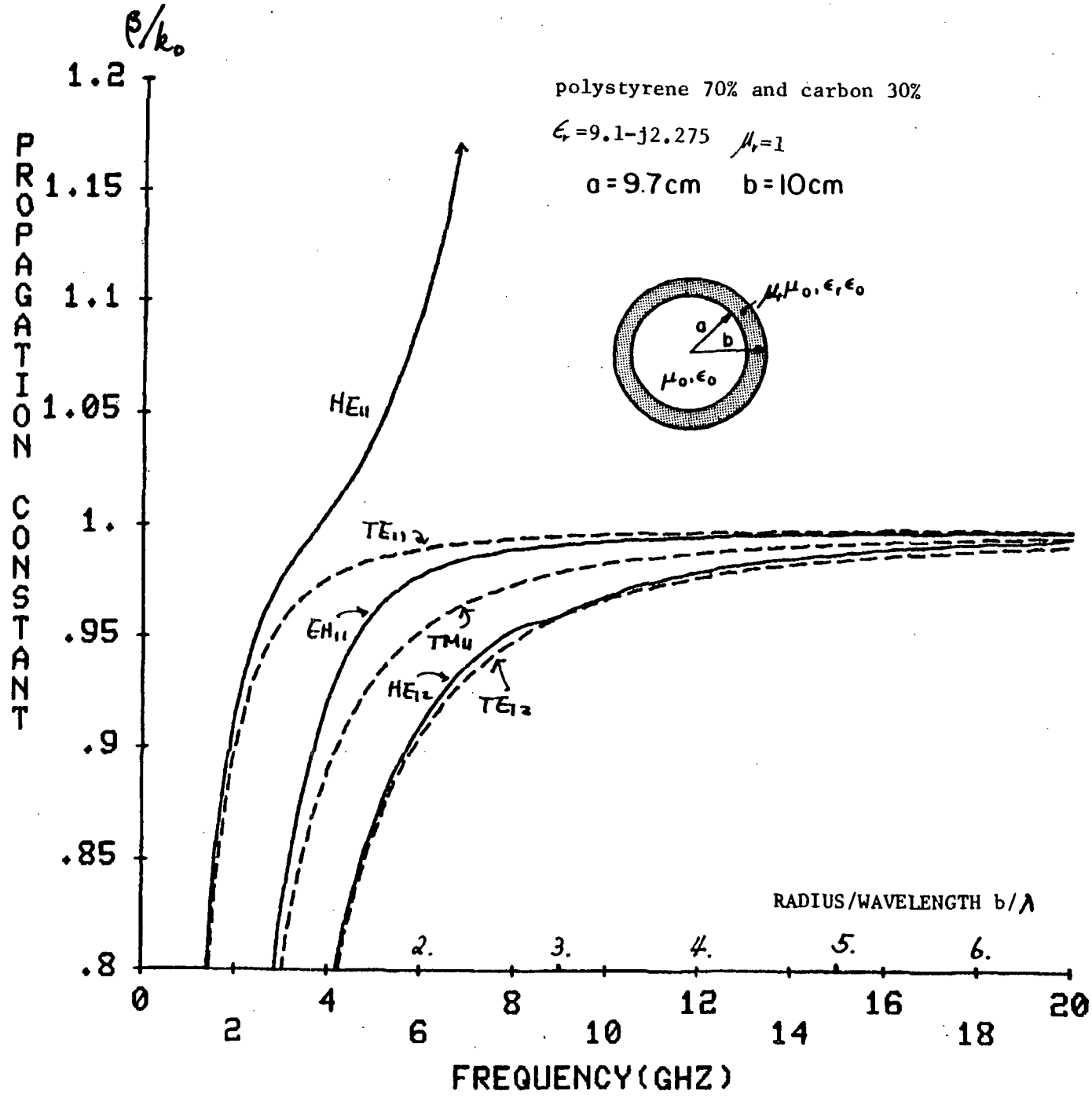

Figure 9. Normalized real parts of propagation constants as a function of frequency (detail) (polystyrene 70% and carbon 30%, $\epsilon_r = 9.1 - j2.275$).

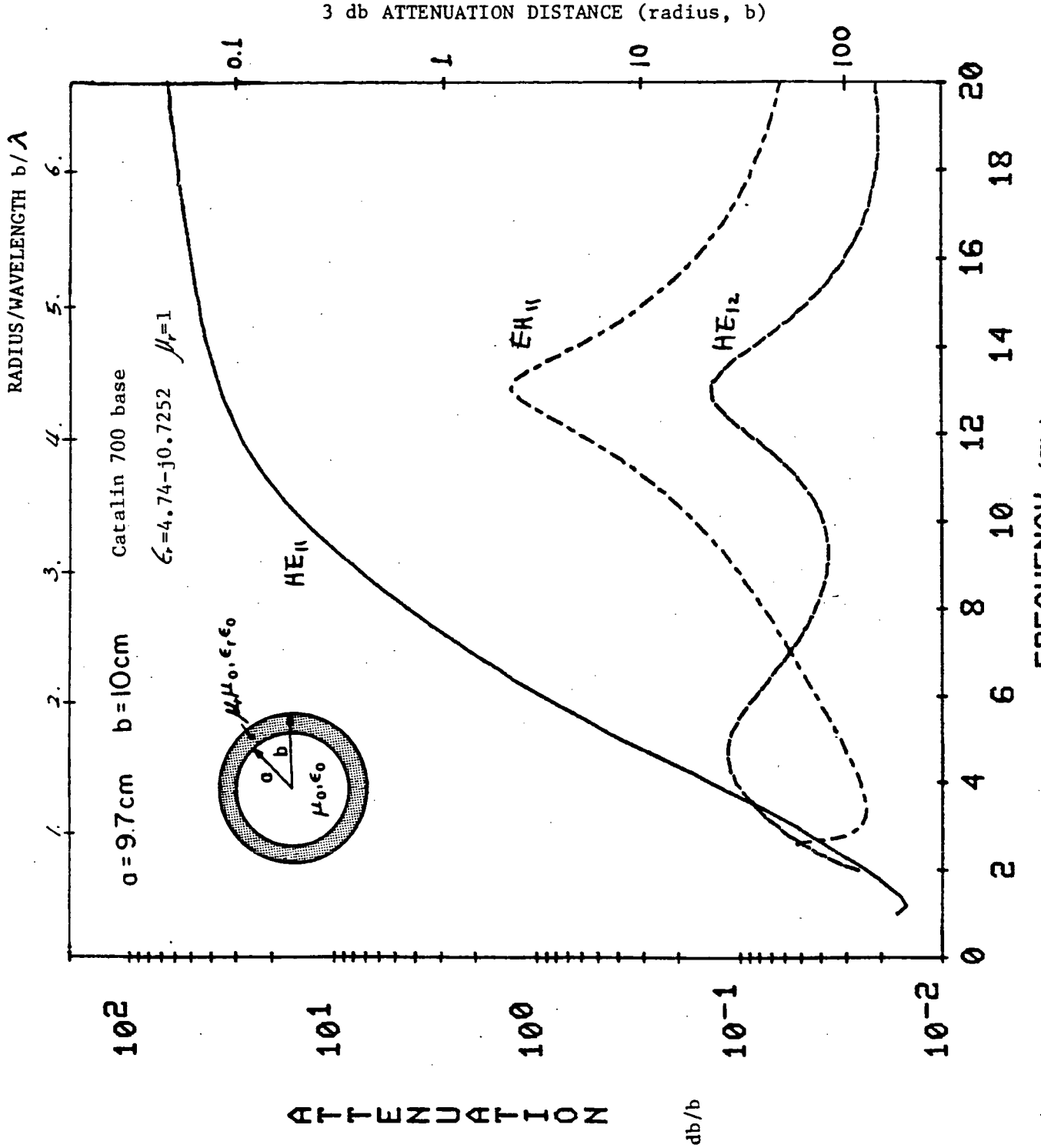

Figure 10. Attenuation constants as a function of frequency (Catalin 700 base, $\varepsilon_r = 4.74 - j0.7252$).

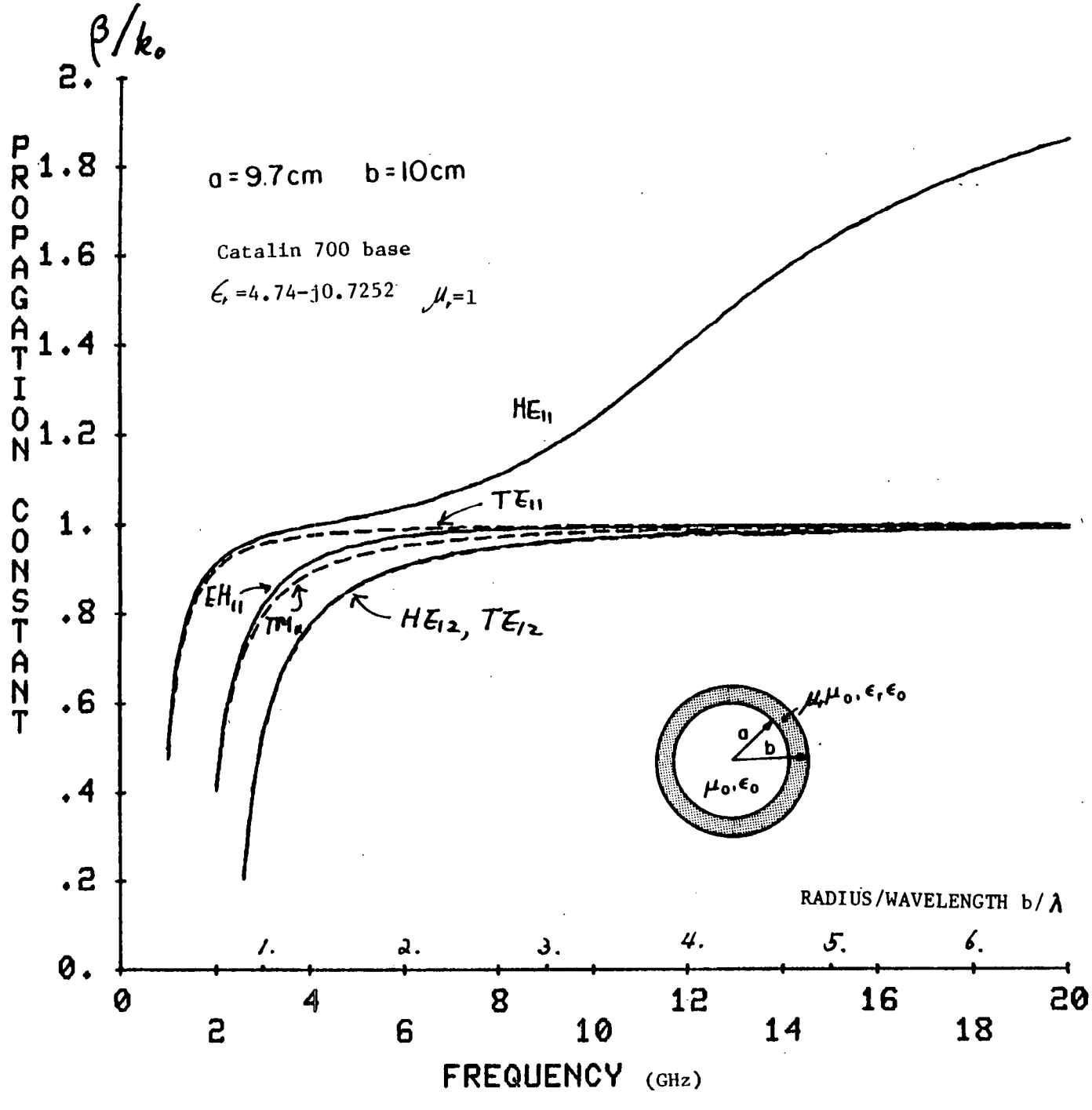

Figure 11. Normalized real parts of propagation constants as a function of frequency (Catalin 700 base, $\varepsilon_r = 4.74 - j0.7252$).

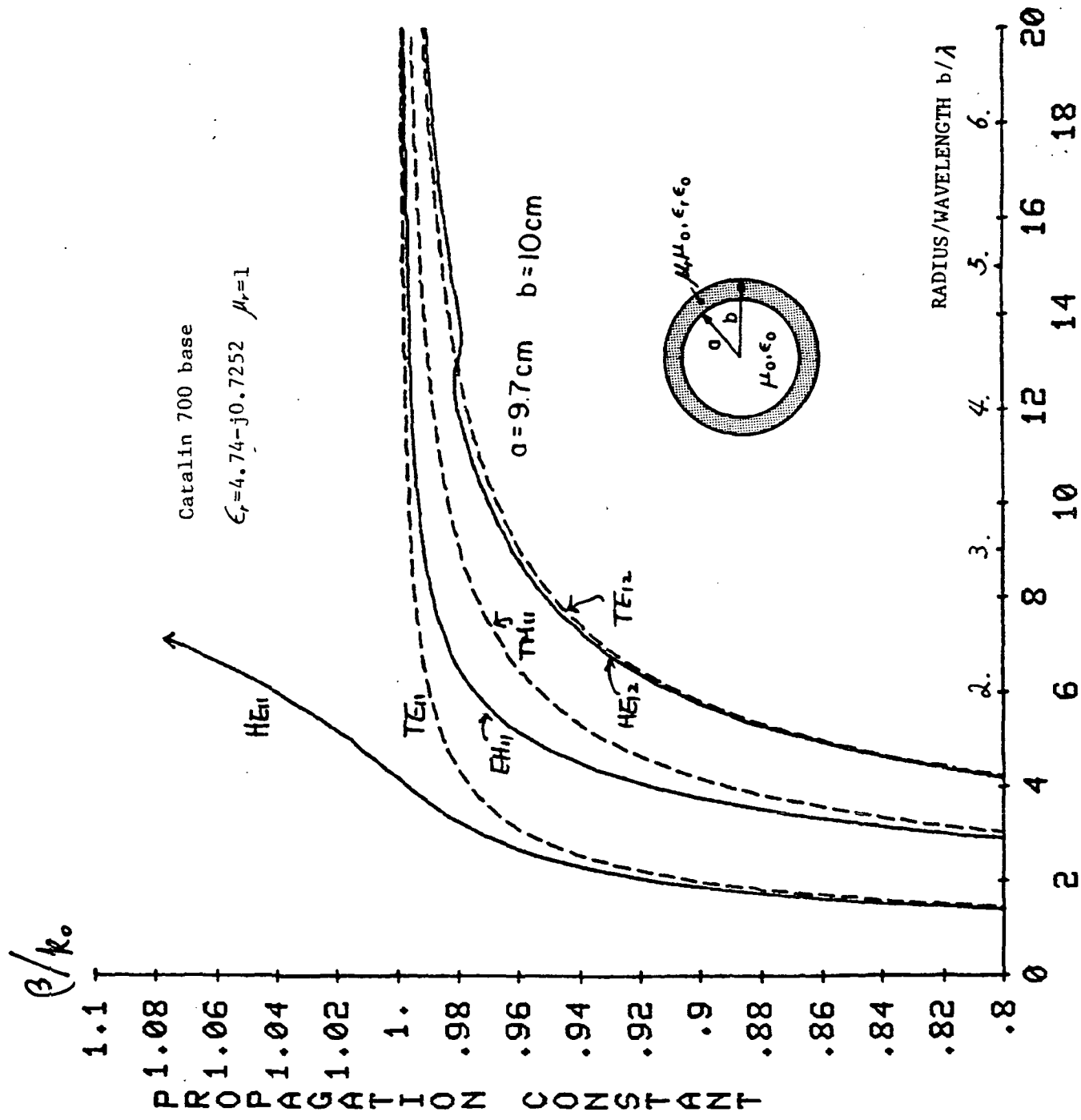

Figure 12. Normalized real parts of propagation constants as a function of frequency (detail) (Catalin 700 base, $\epsilon_r = 4.74 - j0.7252$).

At low frequency, we can easily predict the overall wave attenuation because the dominant mode usually carries most of the transmitted power and the α of the dominant mode usually indicates the overall wave attenuation [4]. On the other hand, at high frequency, the importance of the dominant mode decreases and it is difficult to tell the overall wave attenuation before a large number of the normal modes are accounted for.

In these specific examples, the 3 dB attenuation can be achieved within the distance of 17 diameters of the cylinder in the waveguide thinly coated with polystyrene 70% and carbon 30% at 3 GHz (a = 9.7 cm, b = 10 cm, (b - a)/b = 3%). The 3 dB-attenuation distance for the waveguide coated with Catalin 700 base (with the same physical parameters as the above) is about 28 diameters of the cylinder. At a higher frequency, it is difficult to predict the 3 dB-attenuation distance $Z_{1/2}$ at this moment, but we can guess from the general patterns of the attenuation constants that the $Z_{1/2}$ would not be much different from that at the frequency of 3 GHz.

Another interesting feature of the attenuation constants in Figures 7 and 10 is the presence of the peaks of the EH_{11} and HE_{12} modes, which are not present in the previous hypothetical example (Figure 4). We expect these peaks are due to the spatial resonance because these peaks occur when the phase distance of the thickness of the dielectric layer is roughly $\pi/4$.

In the paper reported earlier [4], we investigated the asymptotic behavior of the attenuation constants of the normal modes in the lossy waveguide as a function of the imaginary part ε_r^I of the dielectric constant ε_r. At the time when that report was written, we could not complete the calculation because a numerical difficulty similar to that at high frequency was encountered in the computer programming. With the modified version of our program, we can get a complete picture of the general trend of

α as a function of ε_r^I (Figure 13). The peak at the smaller ε_r^I is due to the dielectric resonance. This dielectric-resonance peak disappears when ε_r^R is large ($\varepsilon_r^R \gtrsim 2$) [1], [4]. The interesting feature in this figure is the second peak at a large ε_r^I. This peak is believed to be due to the spatial resonance because this peak occurs when the layer thickness is about 1/4 wavelength within the dielectric layer. A similar result was reported earlier when we varied the layer thickness [1], [4]. From these results, we can draw an important finding: The optimum thickness of the lossy dielectric layer for maximum wave attenuation is about 1/4 wavelength. In other words, coating the cylinder thicker than 1/4 wavelength would be counter-productive in attaining a large wave attenuation in the lossy waveguide.

We also investigate the wave attenuation in the waveguide coated with a lossy magnetic material. Before we choose any practical material for the lossy magnetic material, we first studied the general properties of the attenuation constant as functions of frequency and the magnetic permeability of the lossy magnetic material.

Figure 14 shows the attenuation constants α's as a function of frequency when the waveguide is coated with a lossy magnetic material which has the same numerical value of the magnetic permeability as that of the dielectric constant in Figure 4 for the purpose of comparison. We observe a few interesting features in this figure compared to that in Figure 4 where the waveguide is coated with a lossy dielectric material. First, the waveguide coated with the magnetic material has a much larger α than that with a lossy dielectric. We can explain this result with the idea of the quasi-static approximation [8]. In the lossy dielectric material, the power loss is

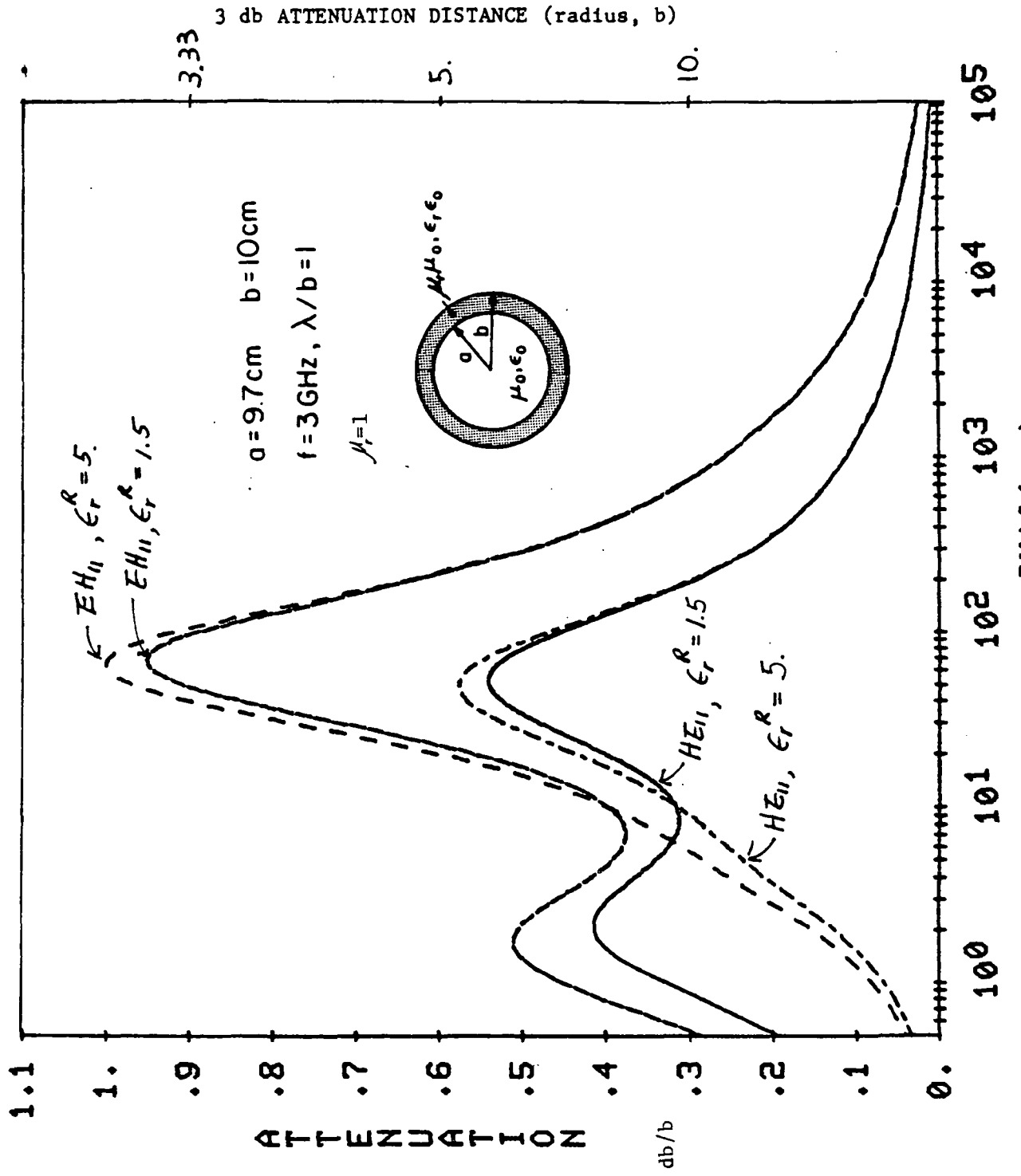

Figure 13. Attenuation constants as a function of the imaginary part of the dielectric constant (f = 3 GHz).

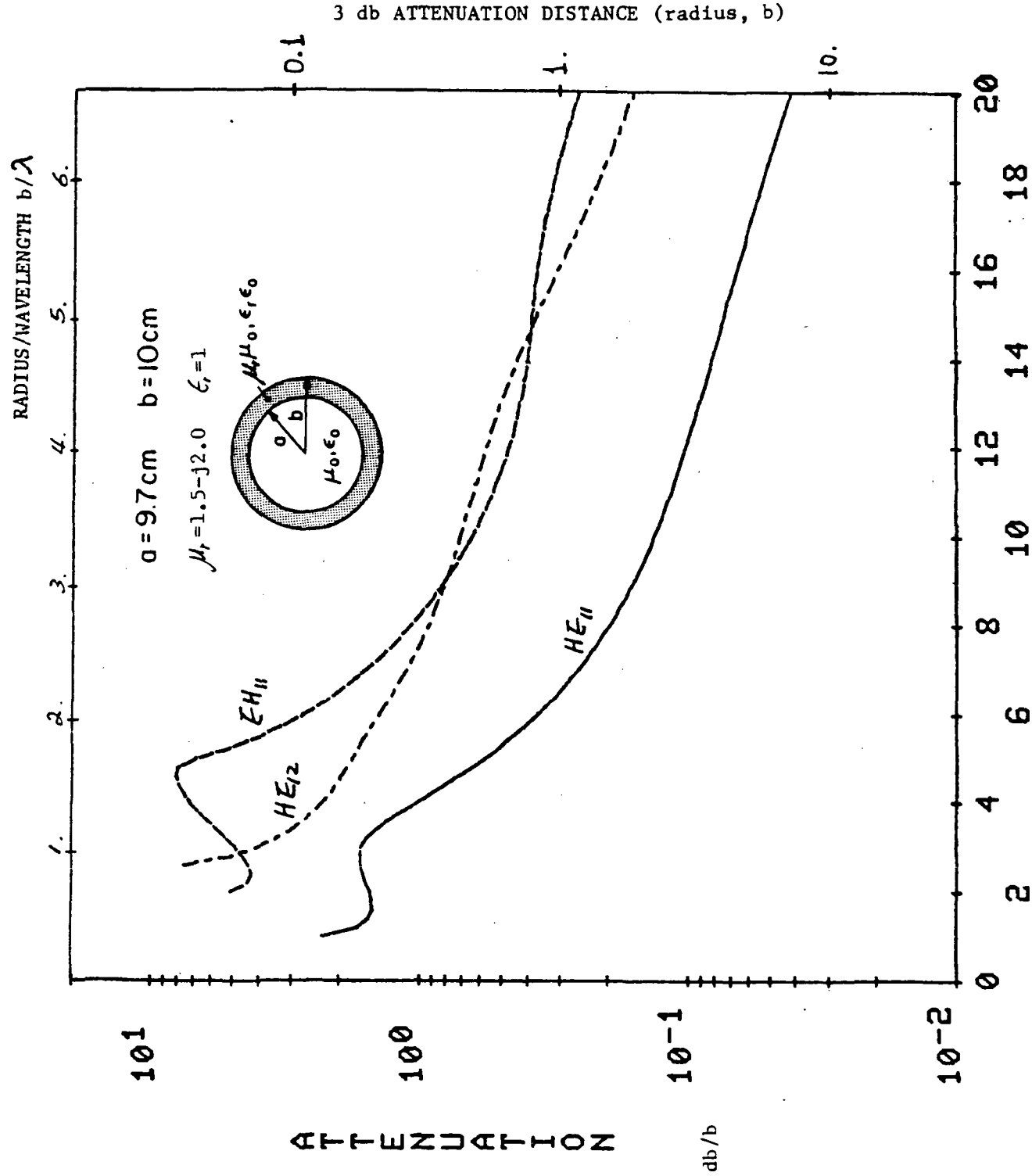

Figure 14. Attenuation constants as a function of frequency (μ_r = 1.5 - j2.0).

related to the electric energy of the wave. On the other hand, the power loss in the lossy magnetic material is related to the magnetic energy. When the surface of the cylinder is perfectly conducting as in our problem, the magnetic energy stored in the lossy material around the conducting surface is much larger than the electric energy because the tangential component of the electric field vanishes on the perfectly conducting surface. Therefore, we expect that placing a lossy magnetic material around the conducting wall produces much larger wave attenuation than placing a lossy dielectric material there.

At high frequency, this quasi-static argument breaks down. In fact, we observe that the attenuation constants of the normal modes decrease very rapidly as frequency increases. Also, we observe that the real parts, β's, of the propagation constants of the normal modes approach those of the unperturbed waveguides (Figures 15 and 16). We also notice that there is a clear mode coupling. However, we do not have a satisfactory answer to why the β's of the normal modes behave in this way.

It is interesting to note that there is no "surface-mode" anomaly and the dominant mode has a smaller α than the other two modes in contrast to the case in the waveguide coated with lossy dielectric material (Figure 4).

Next we investigate the α as a function of the imaginary part μ_r^I of the magnetic permeability (Figure 17). The α of the dominant mode (HE_{11}) is fairly constant for the loss tangent larger than 1, though there is a slight decreasing trend of the α as the μ_r^I increases. The α's of the higher modes (EH_{11} and HE_{12}) are much larger than that of the dominant mode, and show strong resonance peaks. Why such maxima exist is not yet clear. It is interesting to note that the peaks occur where the β's of two

ORIGINAL PAGE IS
OF POOR QUALITY

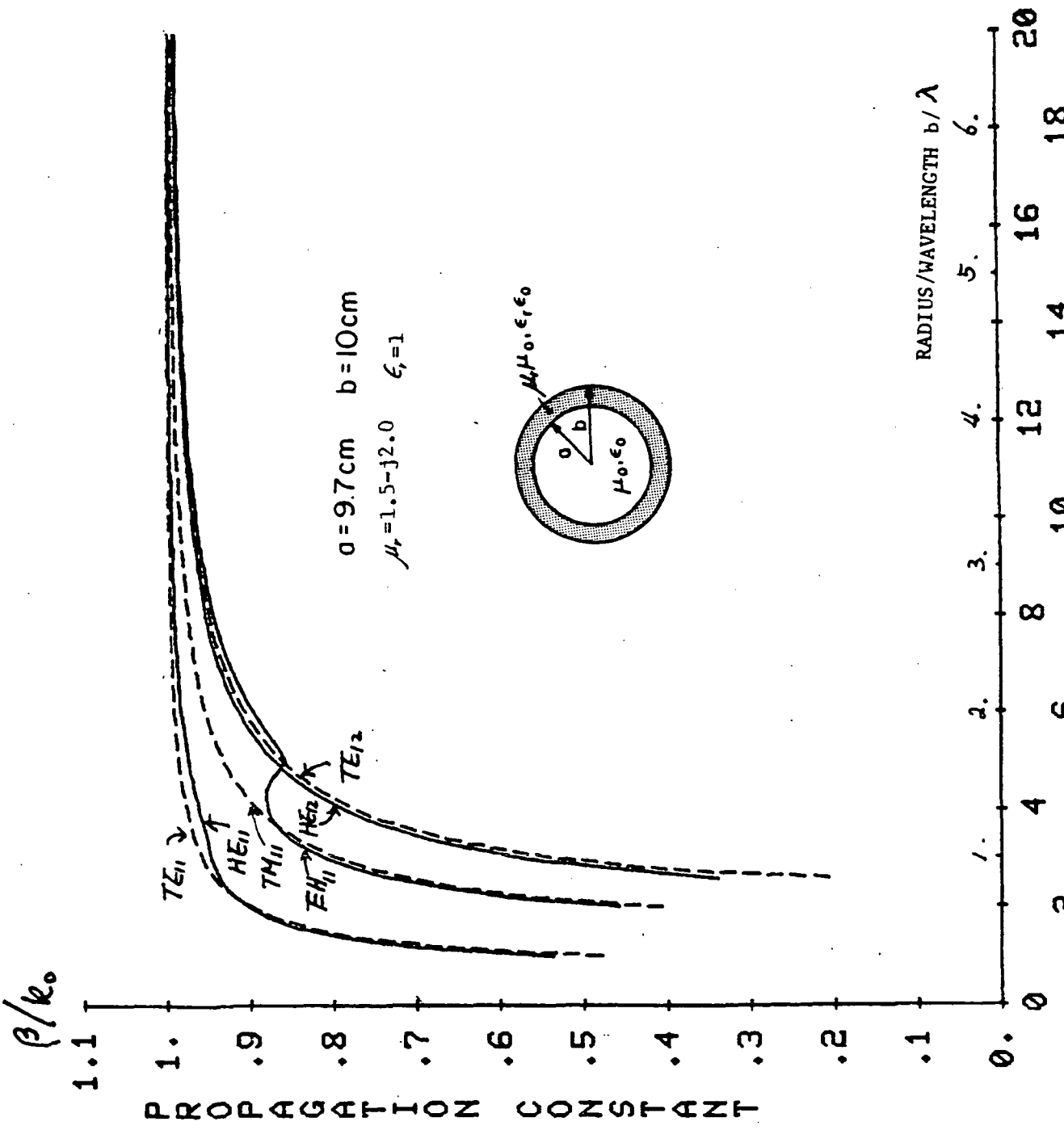

Figure 15. Normalized real parts of propagation constants as a function of frequency (μ_r = 1.5 - j2.0).

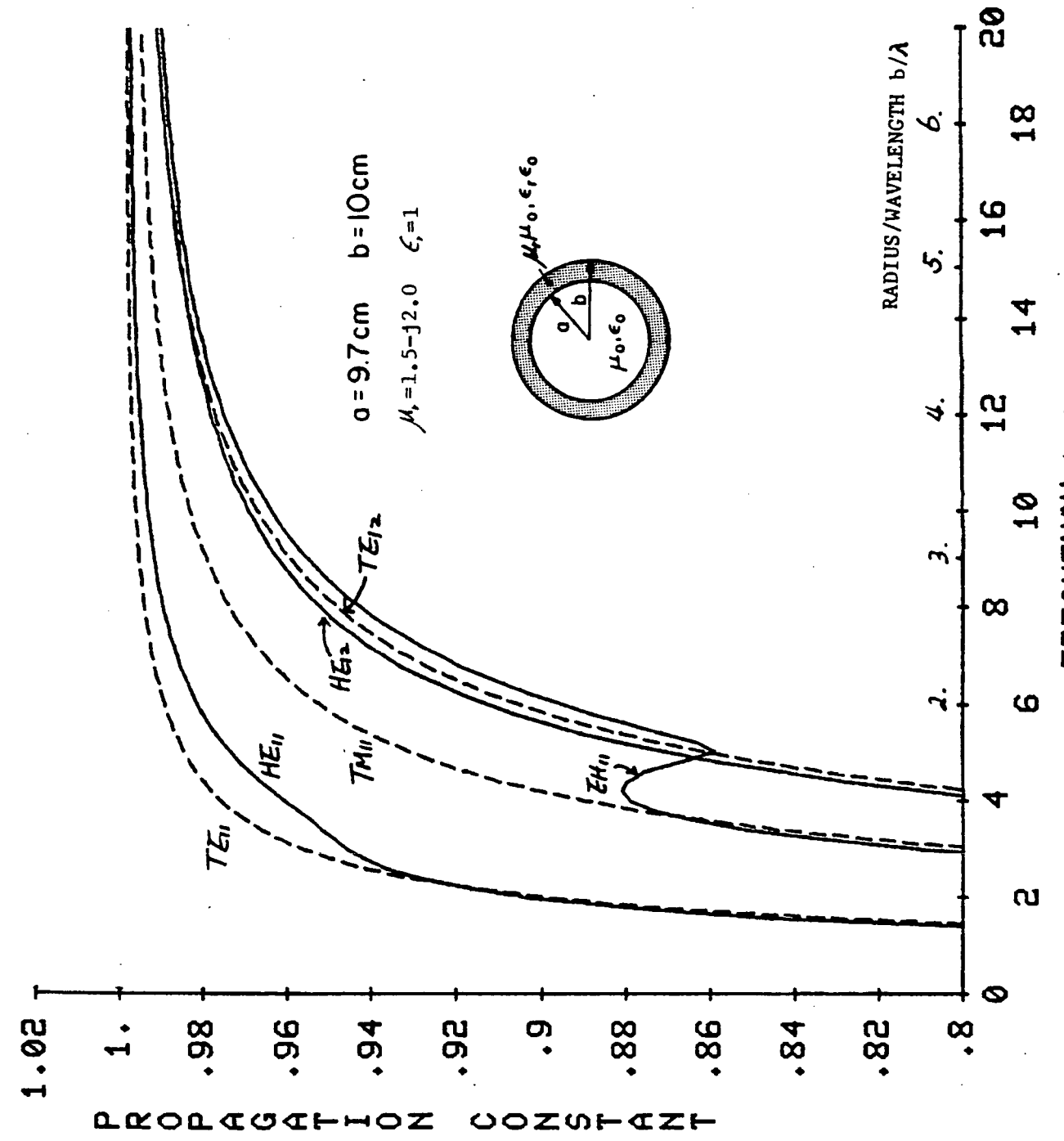

Figure 16. Normalized real parts of propagation constants as a function of frequency (detail)(μ_r = 1.5 - j2.0).

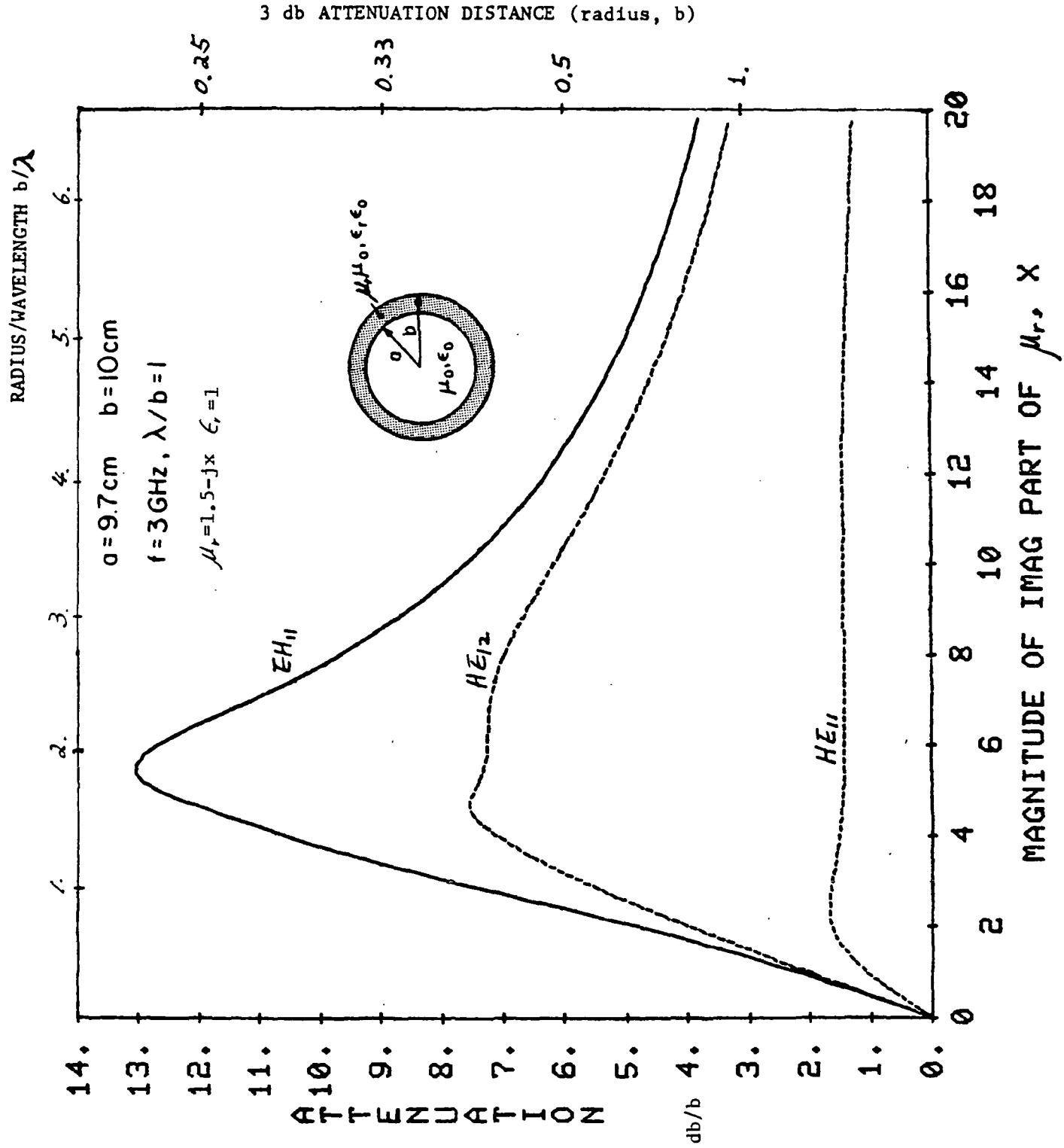

Figure 17. Attenuation constants as a function of the imaginary part of the magnetic permeability ($\mu_r^R = 1.5$, f = 3 GHz).

higher modes (EH_{11} and HE_{12}) become degenerate. We do not see any hint of the coupling of the dominant mode with other modes (Figure 18).

Figure 19 shows the α as a function of the real part of μ_r^R of the magnetic permeability. The α of the HE_{11} mode increases very rapidly as the μ_r^R increases. On the other hand, the α's of the HE_{11} and EH_{12} modes decrease very rapidly for the loss tangent larger than 1 as the μ_r^R increases. Figure 20 shows the β's of the normal modes. From this figure, we see clearly the HE_{11} mode becomes a surface mode which is confined to a small region of the lossy magnetic material. As indicated previously, this surface mode of HE_{11} is not effective to attenuate the overall transmitted wave, and in this case, the EH_{11} mode becomes the dominant propagating mode, which determines the overall wave attenuation.

From the above results, we can say that the permeability constant of the lossy magnetic material as a good coating material should have large values of both μ_r^R and μ_r^I, but the loss tangent should not be much larger than 1.

With the above information, we choose the two best materials we can find for further analysis, namely, Crowly BX113 (μ_r = 1.74 - j3.306, ε_r = 12 - j0.144) and Ferramic B(μ_r = 0.29 - j2.9, ε_r = 20 - j 13.6) [7]. The α and β for Crowly BX113 are shown in Figures 21, 22, and 23, and those for Ferramic B in Figures 24, 25 and 26. Even though there are large differences in both ε_r and μ_r, the general dependences of the α's and β's on frequency for those two examples and the hypothetical example given previously (Figures 14, 15 and 16) are amazingly similar. Especially, the similarity of the general dependences of the α's and β's on frequency in the above cases even with very different values of ε_r suggests that the magnetic permeability of the lossy material has stronger influence on

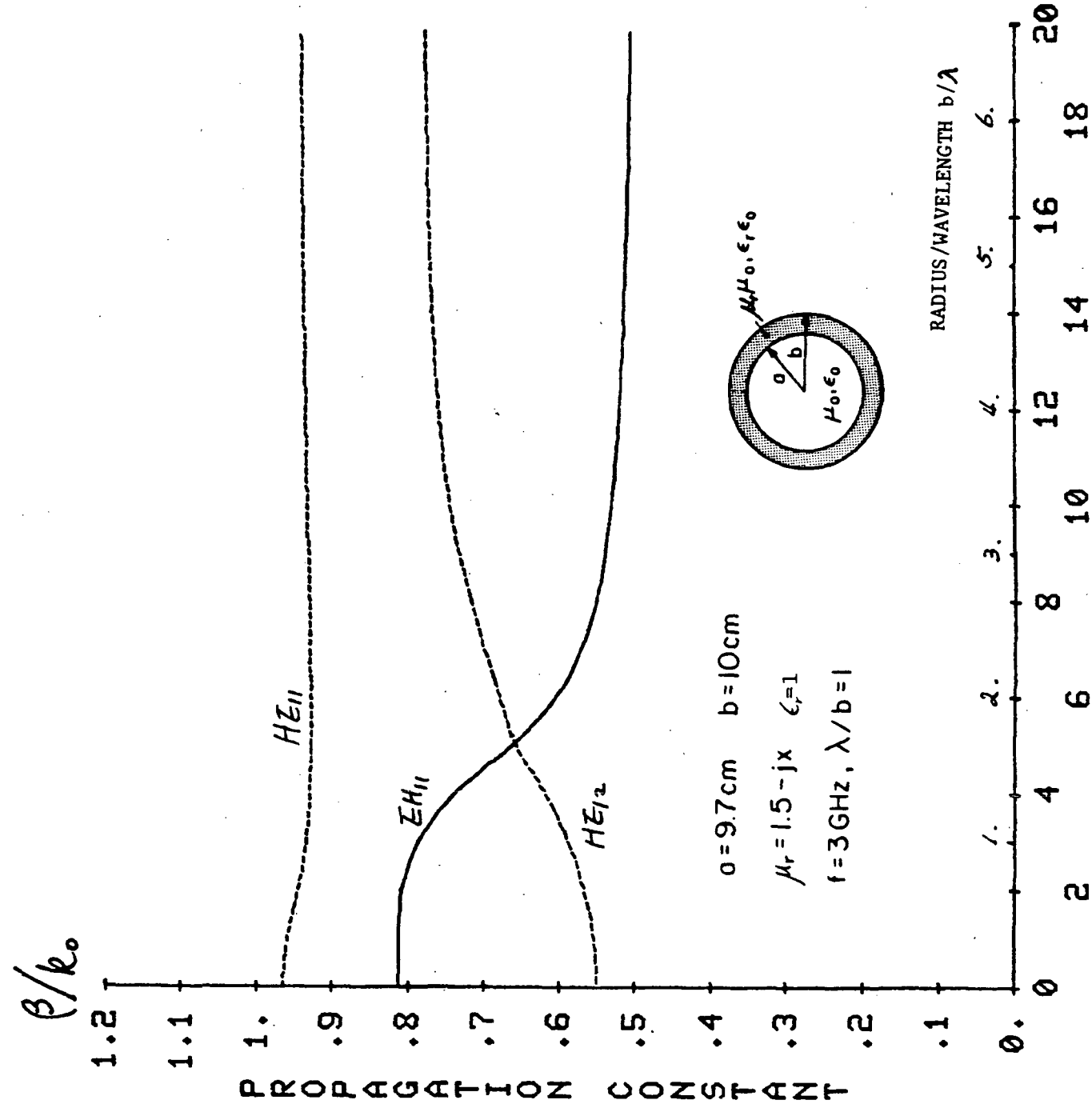

Figure 18. Normalized real parts of propagation constants as a function of the imaginary part of the magnetic permeability ($\mu_r^R = 1.5$, f = 3 GHz).

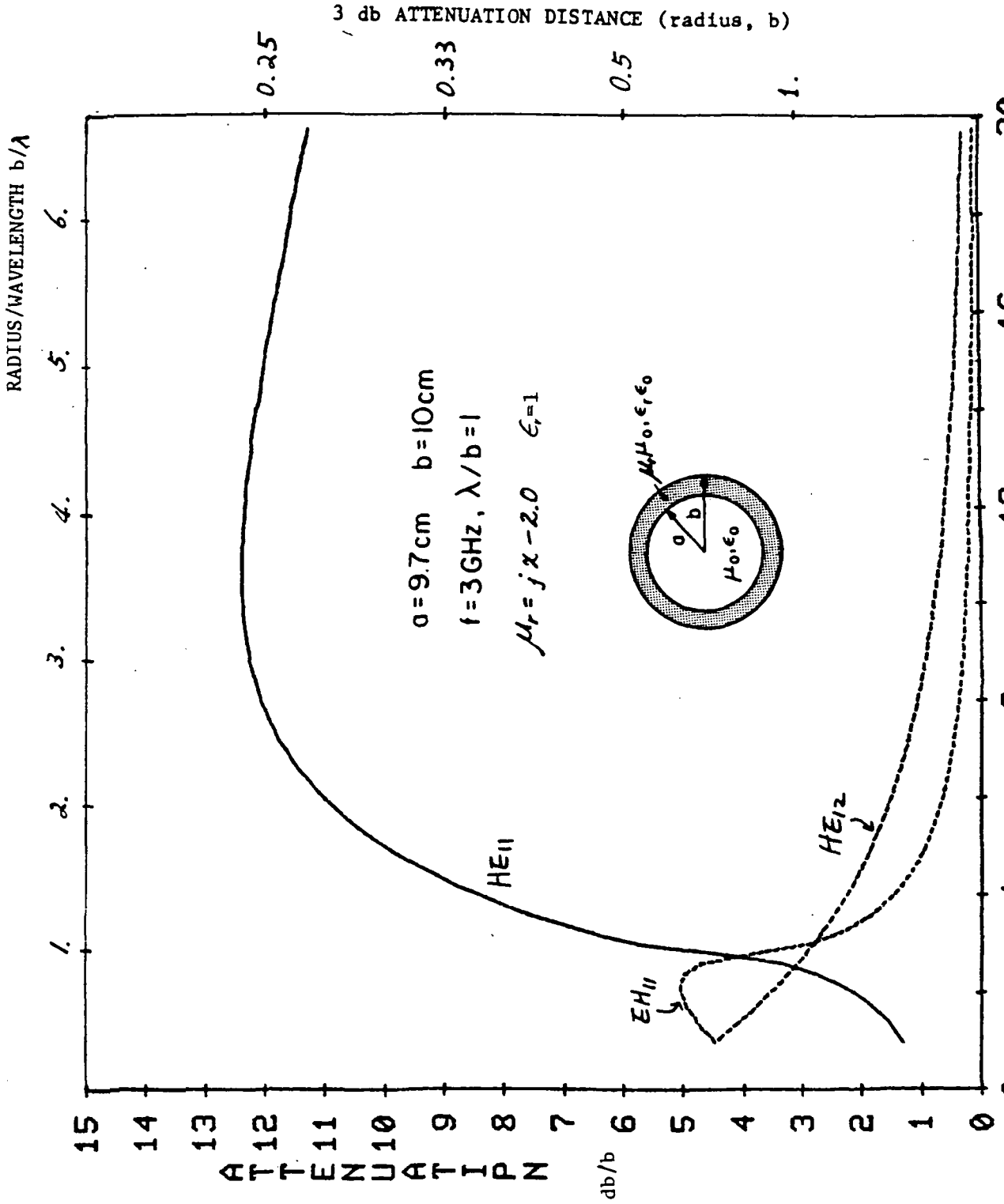

Figure 19. Attenuation constants as a function of the real part of the magnetic permeability (μ_r^R = 2.0, f = 3 GHz).

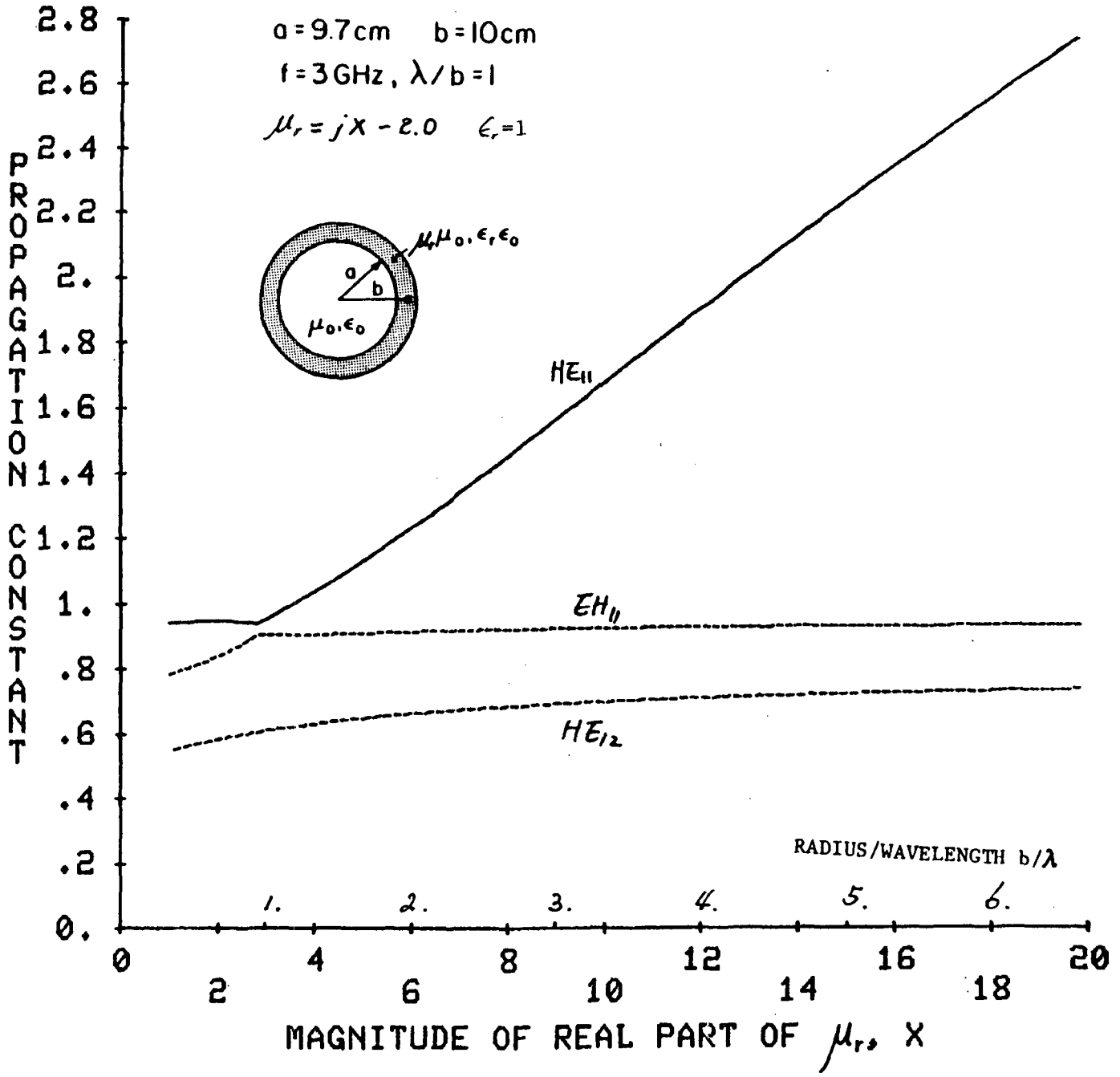

Figure 20. Normalized real parts of propagation constants as a function of the real part of the magnetic permeability (μ_r = 2.0, f = 3 GHz).

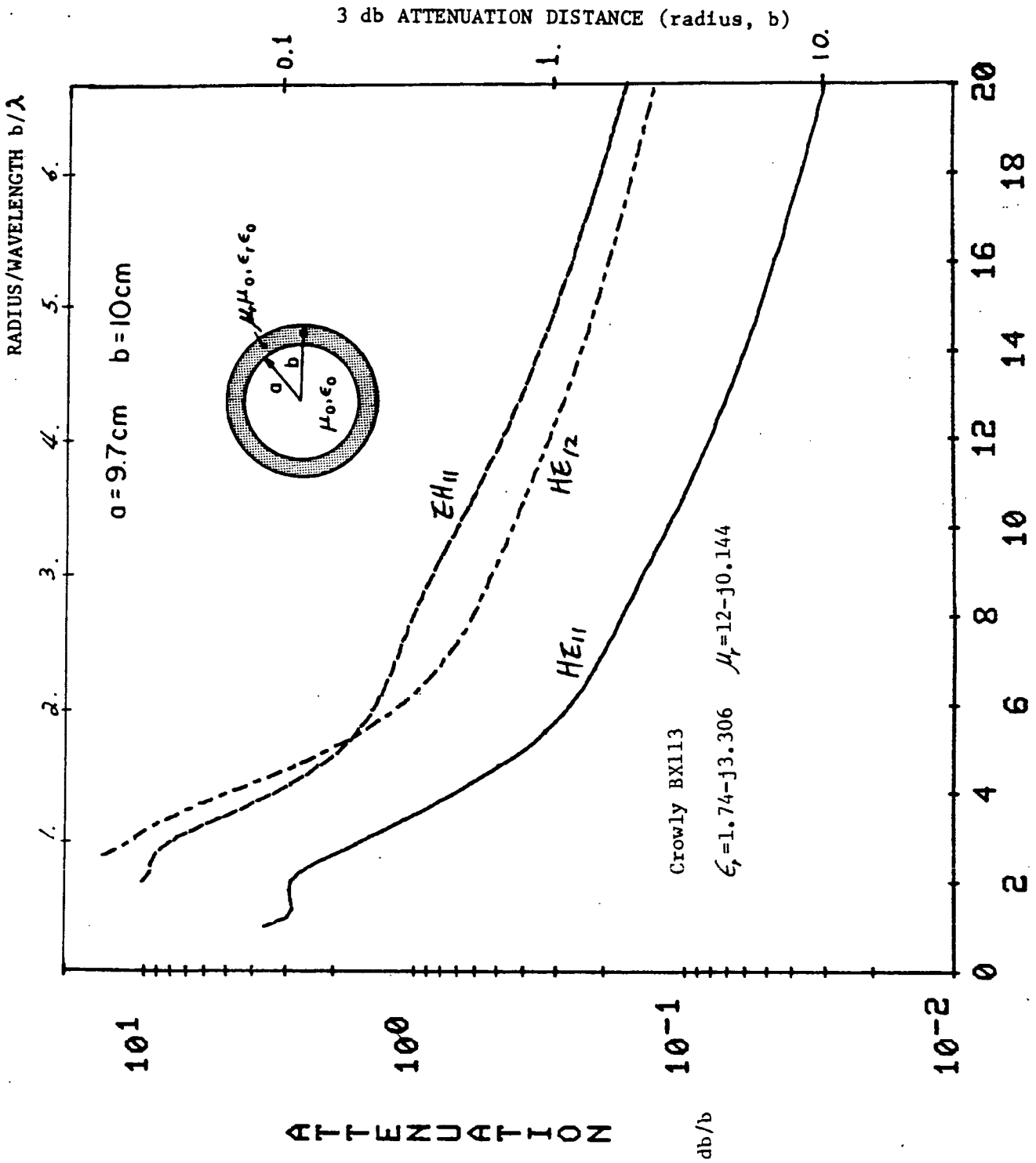

Figure 21. Attenuation constants as a function of frequency (Crowly BX113, $\mu_r = 1.74 - j3.306$, $\varepsilon_r = 12 - j0.144$).

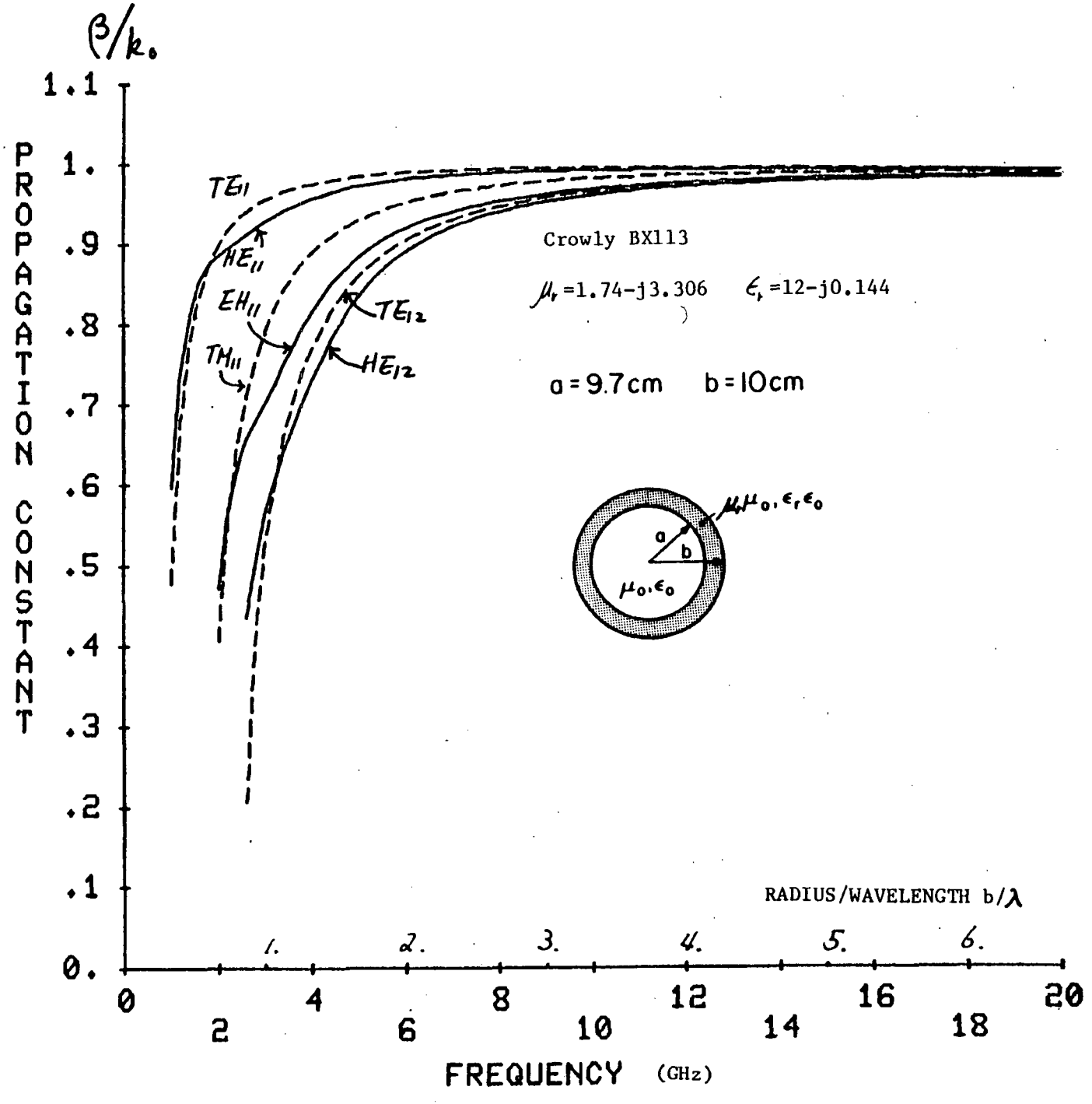

Figure 22. Normalized real parts of propagation constants as a function of frequency (Crowly BX113, $\mu_r = 1.74 - j3.306$, $\varepsilon_r = 12 - j0.144$).

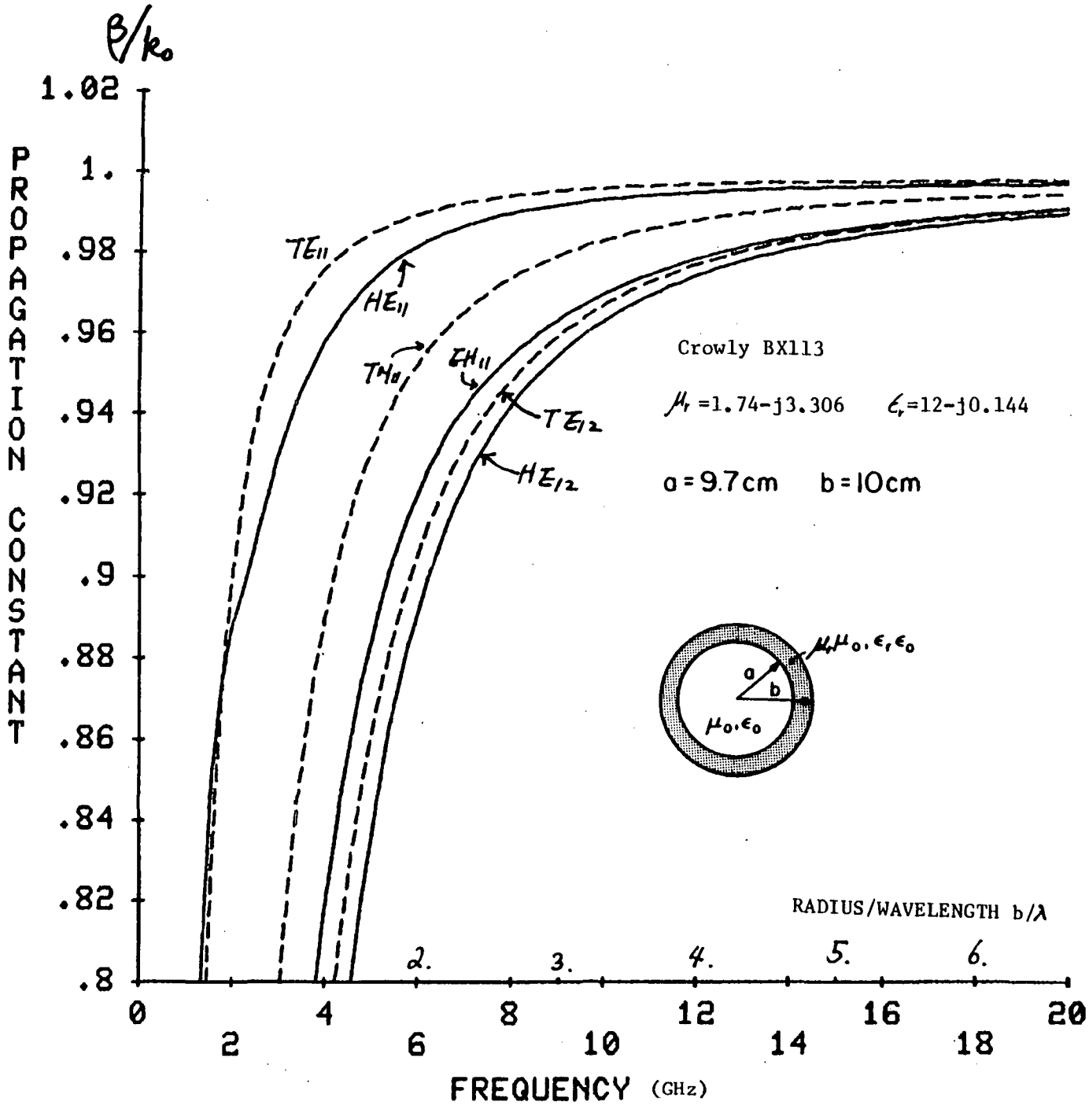

Figure 23. Normalized real parts of propagation constants as a function of frequency (detail)(Crowly BX113, $\mu_r = 1.74 - j3.306$, $\varepsilon_r = 12 - j0.144$).

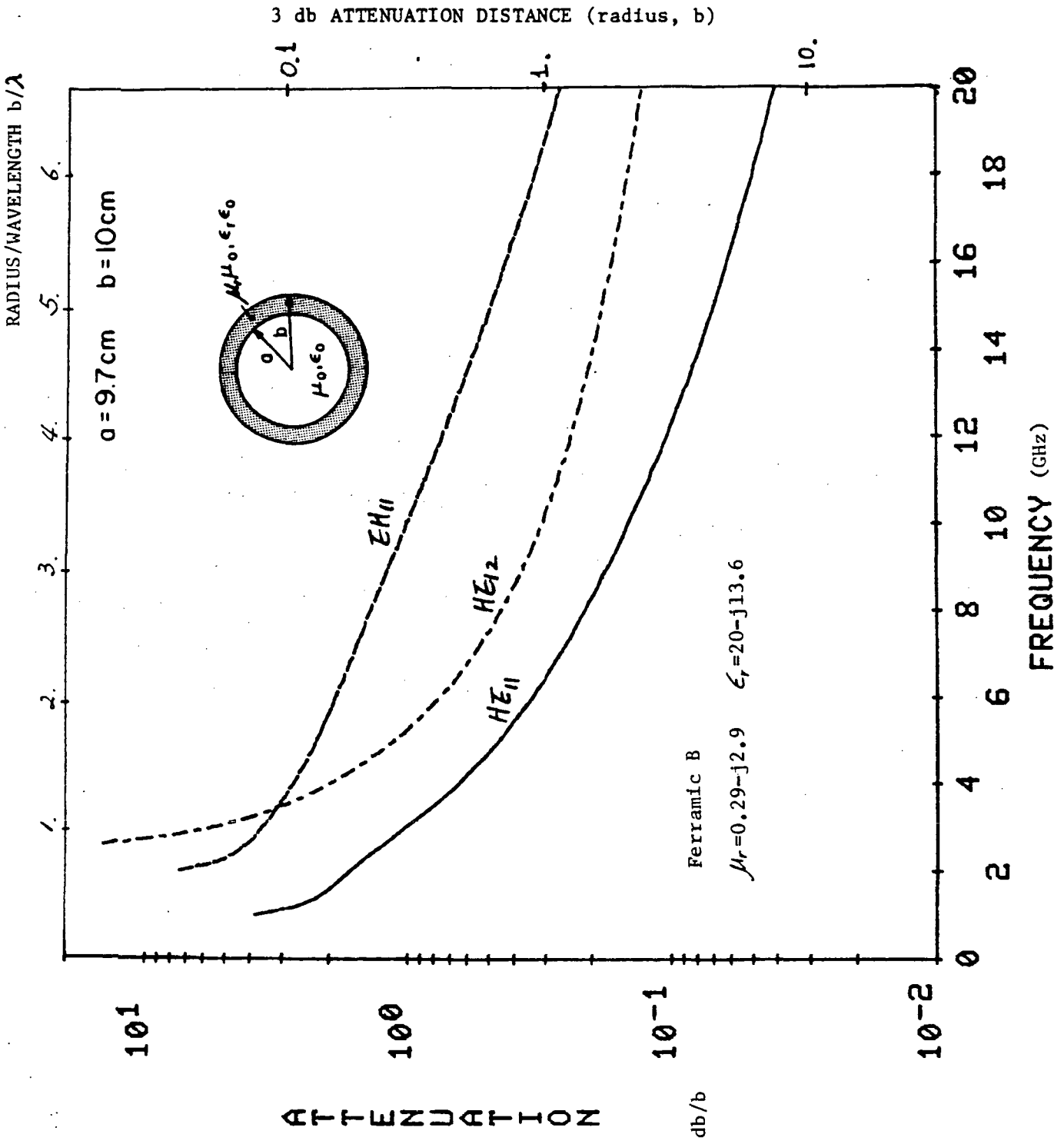

Figure 24. Attenuation constants as a function of frequency (Ferramic B, $\mu_r = 0.29 - j2.9$, $\varepsilon_r = 20 - j13.6$).

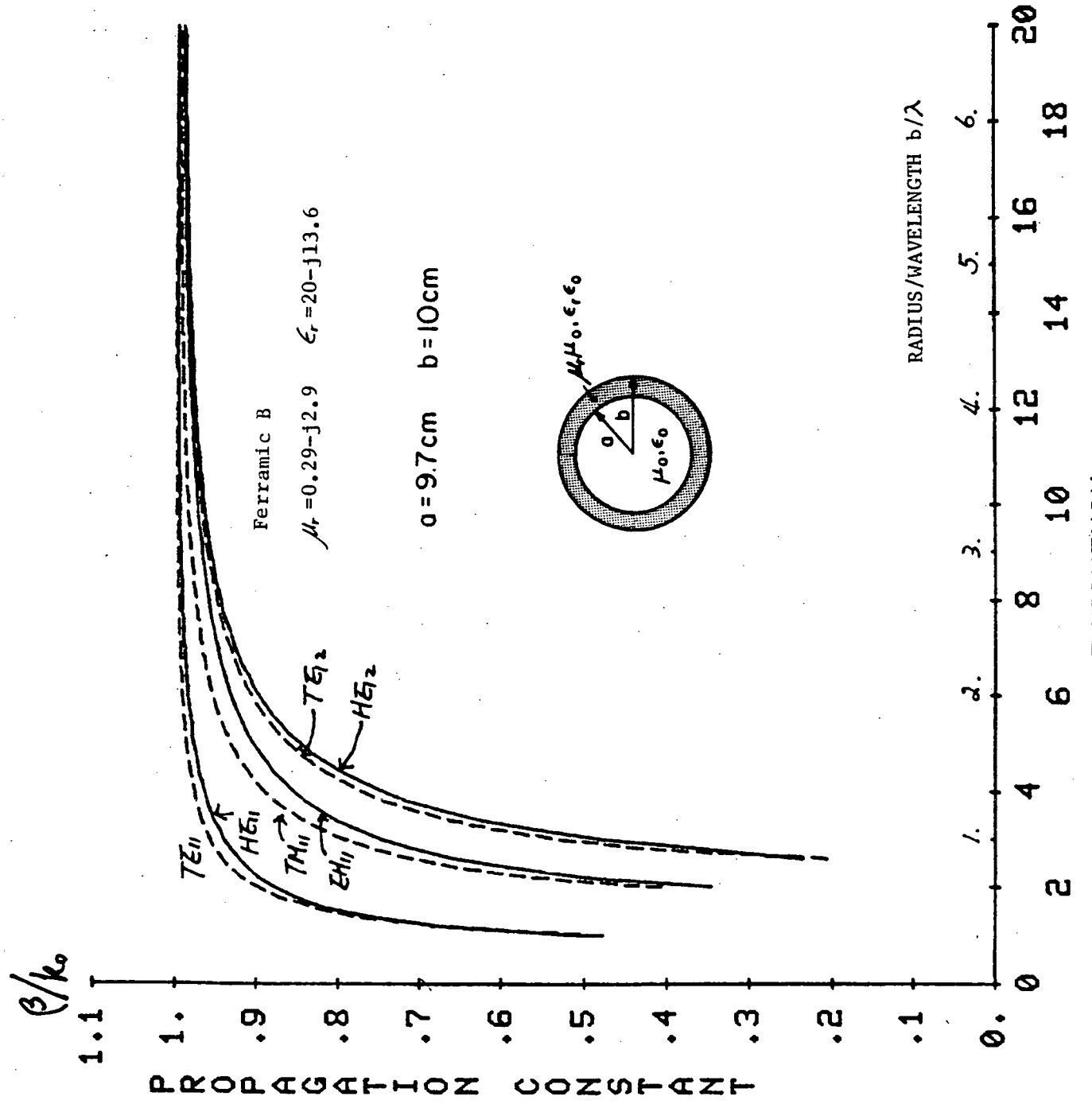

Figure 25. Normalized real parts of propagation constants as a function of frequency (Ferramic B, $\mu_r = 0.29 - j2.9$, $\varepsilon_r = 20 - j13.6$).

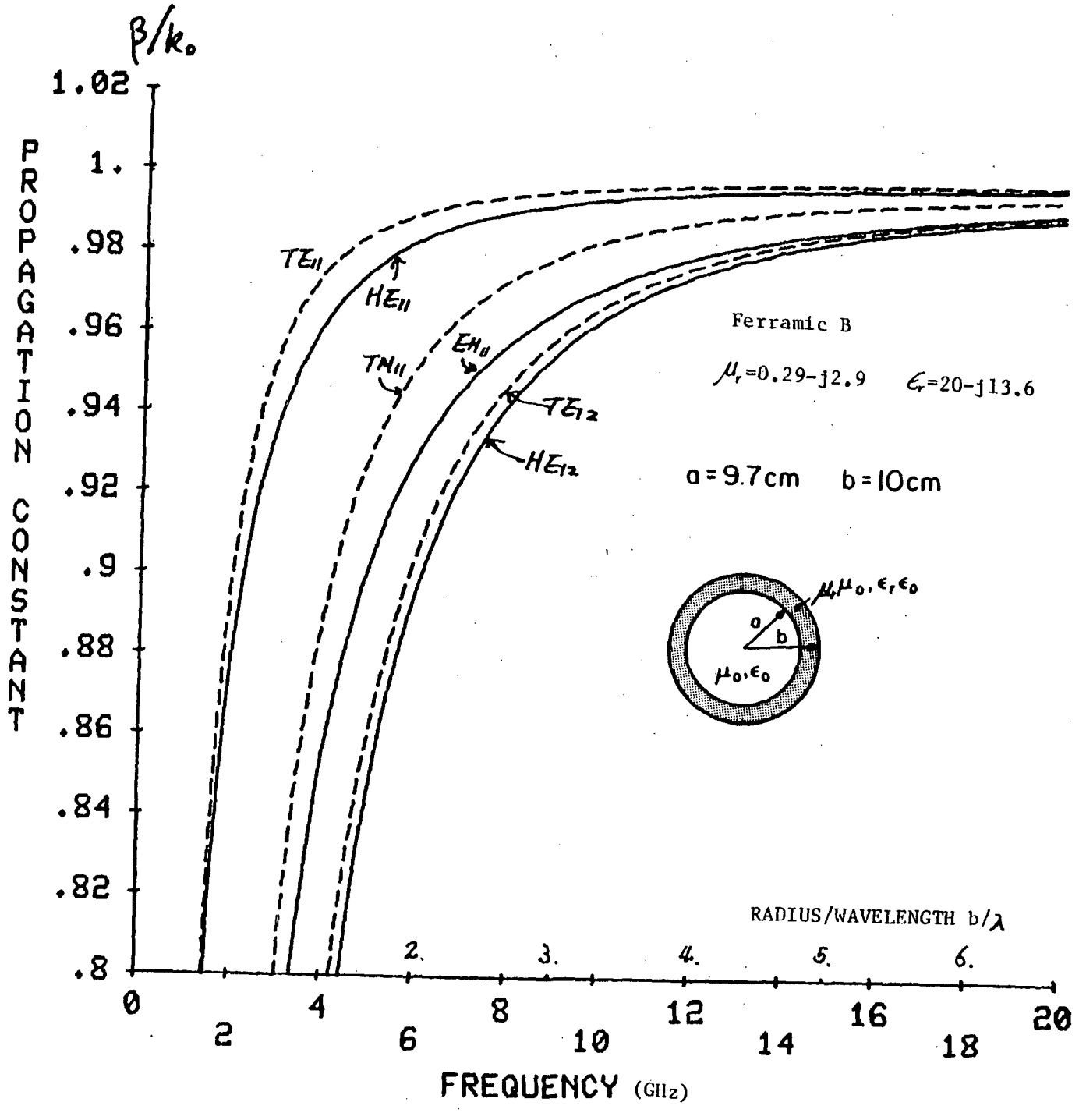

Figure 26. Normalized real parts of propagation constants as a function of frequency (detail)(Ferramic B, μ_r = 0.29 - j2.9, ϵ_r = 20 - j13.6).

shaping the modal fields within the lossy waveguide than the dielectric constant. It is interesting to observe that the α's and β's converge to the values of the α's and β's in the perfect waveguide, but how this happens is not yet clear.

The 3 dB-attenuation distance of the transmitted wave at 3 GHz in the waveguide coated with Crowly BX113 (a = 9.7 cm, b = 10 cm, (b - a)/b = 3%) is about one diameter of the cylinder and the 3 dB-attenuation distance with Ferramic B (with the same physical parameters as with Crowly BX113) is less than 2 diameters. At high frequency, we can not give the exact value of the 3 dB-attenuation distance, but from the figures shown in Figures 21 and 24, the wave attenuations decrease very rapidly as frequency increases.

Finally we summarize as follows.

1) The best material for the dielectric coating has a large loss tangent, and the optimum thickness of the layer is 1/4 wavelength in the dielectric region.

The transmitted wave from the outside illumination into the waveguide thinly coated (a = 9.7 cm, b = 10 cm, (b - a)/b = 3%) with the best lossy dielectric (polystyrene 70% and carbon 30%, $\varepsilon_r = 9.1 - j2.275$) at the low frequency (3 GHz) attenuates to 3 dB within the distance of 17 diameters of the cylinder. At high frequency, the analysis is more complicated, but we do not expect that the 3 dB-attenuation distance is much different from that at the low frequency.

2) The best material for magnetic coating has a large imaginary part of the magnetic permeability, and the loss tangent is not much larger than 1. The lossy magnetic material can be very effective in attaining a large wave attenuation at the low frequency when this material is used as the coating material in the lossy waveguide. The 3 dB-attenuation distance in

the waveguide thinly coated (as in (1)) with the best material available (Crowly BX113) at the frequency less than 3 GHz is less than one diameter of the cylinder. However, the wave attenuates much less at a higher frequency.

3) In order to complete the analysis of the problem at high frequency, we need to evaluate the coupling coefficients of the incident field with the normal modes in the lossy waveguide. This work is in progress using the Kirchhoff's approximation [3]. Eventually, we will evaluate the radar cross section from the lossy waveguide, including the interior irradiation based on the above results and the rim diffraction using the asymptotic Wiener-Hoff solution [9].

4) We have seen that the magnetic material is more efficient at low frequency than high frequency while the electric material can give a very large wave attenuation of the HE_{11} mode, which is the dominant mode at the low frequency. The mixture of the magnetic and electric materials may combine these two desirable effects to produce a large wave attenuation at the large portion of frequency spectrum. Also, utilizing the multilayers of the lossy materials may alter the field patterns within the waveguide to produce a large wave attenuation [4]. These two aspects for increasing the wave attenuation in the lossy waveguide are now under study.

5) At high frequency, the problem is more complicated because more higher-order modes are involved. Since the normal modes are closely spaced and are strongly mixed with one another at high frequency, keeping the normal modes in order becomes very difficult as frequency increases. Thus it is desirable to obtain an approximate solution for the purpose of comparison. At low frequency, we have used the perturbation method based on the quasi-static approximation to obtain an approximate solution of the

problem. Since the quasi-static approximation becomes invalid at high frequency, other types of approximate solutions for the problem at high frequency have been sought. For this, we have chosen the finite-element method which has been proved to be successful in the waveguide problem [10]. This method can be used not only to check the numerical solution based on the root-searching method, but also to provide a more efficient way to evaluate the propagation constants. The utilization of this finite-element method in our problem is in progress.

REFERENCES

[1] Y. T. Lo and S. W. Lee, "Numerical methods for analyzing electromagnetic scattering," Semiannual Report to NASA Lewis Research Center, Cleveland, Ohio, March 1984.

[2] P. J. B. Clarricoats, "Propagation along unbounded and bounded dielectric rods," Part 1 and Part 2, Proc. Inst. Elect. Eng., Mon. 409E and 410E, pp. 170-186, October 1960.

[3] H. R. Witt and E. L. Price, "Scattering from hollow conducting cylinders," Proc. IEE, Vol. 115, pp. 94-99, January 1968.

[4] C. S. Lee, S. L. Chuang, S. W. Lee, and Y. T. Lo, "Wave attenuation and mode dispersion in a waveguide coated with lossy dielectric material," Univ. of Illinois Electromagnetics Laboratory, Urbana, IL, Technical Report No. 84-13, July 1984.

[5] G. N. Tsandoulas and W. J. Ince, "Modal inversion in circular waveguides - Part I: Theory and phenomenology," IEEE Trans. Microwave Theory Tech., Vol. MTT-19, pp. 386-392, April 1971.

[6] G. N. Tsandoulas, "Bandwidth enhancement in dielectric-lined circular waveguides," IEEE Trans. Microwave Theory Tech., Vol. MTT-21, pp. 651-654, October 1973.

[7] A. R. Von Hippel, Ed., Dielectric Materials and Applications. Cambridge, Massachusetts: Technology Press, M.I.T., 1954.

[8] R. F. Harrington, Time Harmonic Electromagnetic Fields. New York: McGraw-Hill Book Co., 1961, Ch. 7.

[9] C. A. Chuang, C. S. Liang, and S. W. Lee, "High-frequency scattering from an open-ended semi-infinite cylinder," IEEE Trans. Antennas Propagat., Vol. AP-23, no. 6, pp. 770-776.

[10] B. M. A. Rahman and J. B. Davies, "Finite-element analysis of optical and microwave waveguide problems," IEEE Trans. Microwave Theory Tech., Vol. MTT-32, January 1984 and references therein.